GROEL/ES BUFFERS ENTROPIC TRAPS IN FOLDING PATHWAY DURING EVOLUTION OF A MODEL SUBSTRATE

Anwar Sadat[1,3,#], Satyam Tiwari[1,3,#], Kanika Verma[1,3], Arjun Ray[1,3], Mudassar Ali[2], Vaibhav Upadhyay[4], Anupam Singh[3], Aseem Chaphalkar[3], Rahul Chakraborty[1,3], Kausik Chakraborty[1,3,$], Koyeli Mapa[1,2,$,≠]

[1] Academy of Scientific and Innovative Research, CSIR-HRDG, Ghaziabad, Uttar Pradesh, India-201002

[2] Department of Life Sciences, School of Natural Sciences, Shiv Nadar University, Dadri, Uttar Pradesh, India- 201314

[3] CSIR-Institute of Genomics and Integrative Biology, Mathura Road, New Delhi, India-110025

[4] National Institute of Immunology, Aruna Asaf Ali Marg, New Delhi, India-110067

[#] Equally contributing first authors

[$] Equally contributing senior authors

[≠]Correspondence: koyeli.mapa@snu.edu.in

Abstract

The folding landscape of proteins can change during evolution with the accumulation of mutations that may introduce entropic or enthalpic barriers in protein folding pathway, making it a possible substrate of molecular chaperones *in vivo*. Can the nature of such physical barriers of folding dictate the feasibility of chaperone-assistance? To address this, we have simulated the evolutionary step to chaperone-dependence keeping GroEL/ES as the target chaperone and GFP as a model protein by an unbiased screen. We find that the mutation conferring GroEL/ES dependence *in vivo* and *in vitro* encode an entropic trap in the folding pathway rescued by the chaperonin. Additionally, GroEL/ES can edit the formation of non-native contacts similar to DnaK/J/E machinery. However, this capability is not utilized by the substrates *in vivo*. As a consequence, GroEL/ES caters to buffer mutations that predominantly cause entropic traps, despite possessing the capacity to edit both enthalpic and entropic traps in the folding pathway of the substrate protein.

Introduction

Mutations in a protein sequence may subtly change either thermodynamics of the folding polypeptide or that of solvent interactions. *In vivo*, mutations that arise spontaneously may lead to problems in the folding pathway or stability of proteins. This, in turn, may make the proteins either non-functional or dependent on molecular chaperones for folding (Chiti & Dobson, 2017; Hartl, 2017)

The most abundant cytosolic chaperone systems in *E. coli*, consist of the Hsp70 system (DnaK/DnaJ/GrpE), the Hsp60 system (GroEL/GroES), Hsp90 (HtpG), Trigger Factor (Tig) and SecB along with other less abundant chaperones and small heat shock proteins. Properties of the substrates assisted by these chaperone systems have been explored by multiple groups.(Calloni et al., 2012; Dunn, Melville, & Frydman, 2001; Houry, Frishman, Eckerskorn, Lottspeich, & Hartl, 1999; Kerner et al., 2005; Knoblauch et al., 1999; Rüdiger, Germeroth, Schneider-Mergener, & Bukau, 1997). While DnaK system binds to many proteins and has the potential to stabilize thermosensitive proteome (Zhao et al., 2019), GroEL/ES binds and helps in the folding of a much smaller subset of proteins (Kerner et al., 2005; Niwa, Fujiwara, & Taguchi, 2016). The mechanisms of substrate targeting to the right chaperone is an active field of research underlining the significance of the conformations adopted by proteins in their non-folded states (Mapa, Tiwari, Kumar, Jayaraj, & Maiti, 2012; Nagpal, Tiwari, Mapa, & Thukral, 2015).

While canonical chaperone-targeting is important for chaperone-dependent wild type proteins, the accumulation of mutations during evolution may create additional substrates requiring chaperone assistance. Can we predict the type of mutations on a GroEL/ES independent protein that would make it GroEL/ES dependent? Mechanistically, some mutations may increase the propensity of formation of non-native contacts (intramolecular or intermolecular) that need to melt before the protein can fold to its native state (enthalpic trap) while other mutations may increase the flexibility of the non-native states, both of which are folding problems at opposite ends of the spectrum. Do different chaperone systems differ in their capacity to edit the two types of mutations?

GroEL/ES system has been shown to be capable of removing entropic trap in its substrates (Chakraborty et al., 2010; Georgescauld et al., 2014). It has also been shown to unfold proteins (Sharma et al., 2008), removing enthalpic traps in the folding pathway. Does the chaperonin possess both these activities *in vivo*? When proteins accumulate mutations which type of mutations would be preferentially accommodated by GroEL/ES? This is difficult to answer with the previous model substrates as neither the authentic substrates (which precludes understanding the mutational steps that led to its chaperone dependence) nor the slow-folding model substrates (that were not evolved for GroEL/ES dependence *in vivo* in an unbiased manner) gave us the

handle to quantitate folding assistance by GroEL/ES *in vivo*. Although, Horovitz group made advances in this direction by identifying that mutations in frustrated sequence regions lead to GroEL/ES dependence *in vivo*, but the biophysical consequence of these mutations on the folding landscape was not investigated (Bandyopadhyay et al., 2017).

To address this, we sought an unbiased screen using mutagenesis to obtain an *in vivo* GroEL/ES substrate starting from a spontaneously folding GroEL/ES-independent substrate. We show that the identified substrate is exclusively dependent upon the GroEL/ES system *in vivo* and *in vitro*. We find that the unique mutation present in the pool of GroEL/ES dependent protein resulted in an entropic trap in folding that is corrected by GroEL/ES system. We also show that DnaK/DnaJ/GrpE system or the GroEL chaperone can take care of enthalpic traps effectively *in vitro* in an ATP dependent manner, however this function of GroEL is essential for folding the substrate protein *in vivo*. Thus, we posit that proteins that acquire entropic traps during evolution would be assisted by GroEL/ES system *in vivo*. While GroEL/ES also possesses the capability to edit folding landscape by preventing the formation of non-native contacts, this chaperoning capacity is not exclusive to GroEL/ES but is also shared by more abundant DnaK/DnaJ/GrpE system.

Isolation of synthetic GroEL-dependent substrate

Single mutational steps may make a spontaneously folding protein chaperone-dependent during evolution. In order to learn the physico-chemical basis of the mutational step that confers chaperone-dependence, we wanted to mimic this evolutionary step and develop a synthetic substrate dependent on the canonical chaperone GroEL/ES *in vivo* from a GroEL/ES-independent protein. Comparison of the mutant and Wt protein would help in understanding the type of folding problems that GroEL/ES tends to edit, and the mechanism of its chaperoning action. We chose yeGFP (yeast enhanced GFP- referred to as Wt GFP hereafter), a fast folding form of GFP, as the starting protein as, 1) folding of the Wt protein was independent of GroEL/ES *in vivo* and *in vitro* (Figure 1A), and 2) it was easy to quantify the amount of soluble well-folded protein in single-cells using flow-cytometry (Verma et al., 2019). Importantly, to normalize for expression levels, plasmid copy number and induction, we used a Wt mCherry in an operonic construct containing Wt GFP followed by ribosome-binding-site (RBS) and Wt mCherry, under the control of an arabinose-inducible system (Figure 1B). The expression levels of mCherry were used as a reference to obtain the relative expression levels of GFP.

In order to make a GroEL/ES dependent substrate, we generated a random mutant library of GFP using the backbone of this GFP-mCherry operonic construct. The mutant library showed populations of cells containing varying degrees of GFP fluorescence starting from very low

fluorescence to near-native fluorescence (Figure 1C, upper panel). Using fluorescence assisted cell sorting (FACS) we first purified a population of clones (Population-LF) that exhibit extremely low GFP fluorescence compared to Wt GFP (Figure 1C). These clones would either have problems in folding or have quenched fluorescence due to alteration of fluorophore environment. We co-transformed Population-LF in a K-12 strain of *E. coli* (BW35113, referred to as WT hereafter) overexpressing GroEL/ES from a plasmid under the control of an IPTG-inducible *tac* promoter. We isolated mutant clones that exhibited higher GFP fluorescence upon GroEL/ES overexpression (Figure 1D and S1A). GFP-mCherry plasmids were isolated from individual clones after sorting and re-transformed to confirm the dependence of GFP fluorescence on the overexpression levels of GroEL/ES *in vivo*. Ten of the isolated clones were sequenced and all of them were found to have the mutation K45E; the mutation did not map to any residues around the GFP fluorophore (Figure 1E). The purified mutant protein had similar *in vitro* fluorescence as that of Wt GFP (Figure S1B). *In vivo* fluorescence of K45E mutant (hereafter referred to as slow-folding GFP or sGFP) increased upon co-expression of GroEL/ES (Figure 1F and S1C). The dependence of sGFP on GroEL/ES for folding was further confirmed by the drastic enhancement in solubility of the protein along with GroEL/ES overexpression (Figure 1G). This corroborated well with the increased fluorescence and indicated that sGFP was a folding mutant of Wt GFP that depends upon GroEL/ES system for folding, *in vivo*.

Furthermore, the *in vivo* fluorescence of this mutant did not increase in the presence of DnaK/J/E overexpression (Figure 1H and S1D) or decrease significantly in any of the chaperone deletions (*Tig*, *dnaK*, *dnaJ*) (Figure 1I and S1E). In fact, GFP fluorescence mildly increased in Δ*dnaK,* which is known to overexpress GroEL/ES system (Verma et al., 2019). This suggested that sGFP folding is primarily dependent on the cellular GroEL/ES system. Taken together we find that a single mutation on Wt GFP conferred sGFP with a stringent GroEL/ES dependence, *in vivo.*

To check if K45E confers GroEL/ES dependence specifically or any marginally active mutant of GFP would be GroEL/ES substrate we picked 8 clones randomly from the low fluorescent GFP mutant pool. The basal level fluorescence of these mutants was extremely low and was like that of sGFP. Upon overexpression of GroEL/ES with these mutants only two of the eight mutants showed a GFP fluorescence like that of sGFP in the presence of GroEL/ES (Figure 1J). All the others show lower fluorescence indicating that mutations that confer GroEL/ES dependence is special and is present in ~20% of the mutant pool. That GroEL/ES expression has effect on a small sub-set of the mutant GFP pool, indicates that GroEL/ES most likely rescues only specific problems in folding pathways. K45E mutation captured a rare step that would confer GroEL/ES dependence to a GroEL/ES independent folder such as Wt GFP used in the study.

Refolding of sGFP is limited by a flexibility dependent kinetic trap

To understand the folding barrier that is introduced by K45E, we characterized the spontaneous refolding pathway of sGFP. Wt GFP and sGFP was unfolded in 6M GuHCl for one hour, causing complete unfolding of the protein (Figure S2A) and refolded by a hundred-fold dilution of the unfolded protein in refolding buffer. We found that sGFP refolded with a much slower rate than Wt GFP (Figure 2A) and was fit well to single exponential kinetics (Figure S2B) with an apparent rate of ~$0.2 \times 10^{-3} s^{-1}$.

Next, we checked if sGFP refolding was limited by aggregation. The refolding rate and amplitude of sGFP were independent of the concentration of the protein between 12.5 nM to 400 nM (Figure 2B, S2C, and S2D) proving that neither the refolding rate nor amplitude was limited by off-pathway aggregation. This suggested that the mutation K45E did perturb the unimolecular rate of folding in sGFP.

To understand the type of folding-barrier inserted by the K45E mutation in sGFP, we analyzed the Arrhenius plots for the folding of sGFP and Wt GFP (Figure 2D, Table S2). To account for curvatures in Arrhenius plots of refolding proteins, we fitted temperature-dependent refolding rates of the proteins using a full model of Arrhenius equation containing the $\Delta Cp^{\#}$ term (to account for the difference in heat capacity of the folding intermediate and the transition state) (Dandage et al., 2015). sGFP did not have a temperature-dependent slope suggesting the absence of any enthalpic folding barrier ($\Delta H^{\#}$) while Wt GFP had a high $\Delta H^{\#}$ indicating an enthalpic barrier to folding (Figure 2C, Table S2). Since sGFP refolds slower than Wt GFP, this suggested that the rate-limiting barrier to folding in sGFP is non-enthalpic (Figure S3A). Complementary to $\Delta H^{\#}$ is the value of ρ that is a composite function of the frequency across the transition barrier (prefactor for Arrhenius function) and the entropic assistance towards reaching the transition state (TS) (Figure S3A); lower ρ is associated with higher entropic barrier. ρ is higher for Wt GFP compared to sGFP (Figure 2D, Table S2) demonstrating that the barrier for sGFP folding is entropic in nature. This is consistent with earlier findings with other GroEL substrates (Chakraborty et al., 2010; Georgescauld et al., 2014). sGFP is likely trapped in a folding intermediate I_1 that is stabilized by flexible regions that prevent the formation of native contacts. Analysis of GFP structure reveals that the residue mutated in sGFP, K45, interacted with multiple negatively charged residues in Wt GFP (E32, D210, and E213) (Figure 2E). This lysine residue also formed a core for nucleating long-range interactions in a loop region. The substitution of K45 to a negatively charged glutamate in sGFP could have led to the loss of these interactions and introduced repulsive interactions that would destabilize this region. Spontaneous refolding rate of sGFP increased with an increase in salt concentration (salt shields charges and prevents

repulsive and attractive interactions) (Figure 2F) and charge repulsion in sGFP likely prevented folding by increasing flexibility around this region. Similar salt-dependence was absent in Wt GFP (Figure S2E) demonstrating that substitution of K45 with glutamate introduced electrostatic repulsions that limit sGFP refolding. Taken together, the folding landscape of sGFP has a rate-limiting entropic trap driven by flexibility of I_1 that accounts for the slower folding rate of sGFP compared to Wt GFP.

GroEL/ES alters the folding pathway of sGFP

To check if folding of sGFP was altered by GroEL/ES system, we checked for its chaperone-dependence *in vitro* by reconstituting chaperone-assisted refolding reactions. Refolding of sGFP was strongly accelerated (3~4 fold) by GroEL/ES (Figure 3A) system while that of Wt GFP remained unchanged (Figure 1A). Chaperonin-dependent acceleration was dependent on the presence of all the components; GroEL, GroES, and ATP (Figure 3B). Thus, like authentic class-III (or IV) substrates (Kerner et al., 2005; Niwa et al., 2016) this lab evolved *in vivo* substrate depends on the full-cycle of GroEL/ES system. Moreover, the DnaK/J/E system did not alter the refolding rate of sGFP *in vitro* (Figure S3B) in line with *in vivo* data described earlier (Figure S1D). This demonstrates that the isolated mutant of Wt GFP, sGFP, is a specific substrate of GroEL/ES *in vivo* and *in vitro* and GroEL/ES accelerates the refolding rate of sGFP. A single mutation K45E on Wt GFP confers GroEL/ES dependence on its *in vivo* solubility as well as its refolding rate *in vitro*.

To find the mode of acceleration by GroEL/ES, we obtained the $\Delta H^{\#}$ and ρ for GroEL/ES assisted folding from Arrhenius analysis. Notably, the GroEL/ES system did not decrease the enthalpic barrier ($\Delta H^{\#}$) thereby working through the route of entropic destabilization (Figure 3C, Table S2). A higher value of ρ for GroEL/ES assisted refolding than for spontaneous refolding indicates a lower entropic barrier to refolding in the presence of GroEL/ES (Figure 3C, Table S2). This is consistent with other substrates of GroEL/ES system (Chakraborty et al., 2010; Georgescauld et al., 2014) suggesting that entropic traps in folding landscapes may characterize a GroEL/ES substrate in general, and GroEL/ES could have a general role of affecting entropic destabilization to assist protein folding. The difference in GroEL/ES-assisted and spontaneous refolding pathway is further corroborated with the difference in m-value (dependence of refolding rate on GuHCl concentration) of folding (Figure 3D and 3E).

To check if the allosteric cycle of GroEL/ES or iterative annealing plays a role in accelerating sGFP refolding we used the single ring version of GroEL (SR-EL) (Horwich, Burston, Rye, Weissman, & Fenton, 1998) that lacks the negative allostery between rings, encapsulates the

substrate and completes folding inside the cavity. SR-EL/ES can accelerate the refolding of sGFP like GroEL/ES *in vitro* (Figure S4F) and the Arrhenius parameters (Figure 3D) and m-value (Figure 3E) from SR-EL/ES assisted refolding is similar to that of GroEL/ES-assisted one. This excludes that the temperature-dependent kinetic parameters are independent of temperature-dependent effects on GroEL/ES allostery. Thus, decrease in the entropic barrier of the refolding-substrate is primarily affected by the GroEL/ES cavity and it can rescue the entropically trapped state of the mutant GFP.

GroEL/ES prevents non-native contact formation

Interestingly the yield of spontaneous refolding of sGFP drastically reduced in the absence of any reducing agent in the refolding buffer (Figure4A) and reduced further in the presence $CuCl_2$, a disulfide-assisting catalyst (Figure S4A). Since each molecule of sGFP has two cysteines (C48 and C70) that are distal in the native structure (Figure S4B), there were two possibilities, 1) the proteins formed intermolecular disulfides and formed covalently bonded aggregates or 2) the proteins formed an intramolecular disulfide bond that trapped the molecules in the non-native state. Formation of an intramolecular-disulfide would result in co-migration of two peptides that are disulfide bonded if the protein is digested with trypsin (Figure4B). Mass spectrometry confirmed the presence of the expected product during sGFP refolding in non-reducing condition and proved the formation of an intramolecular-disulfide (Figure 4C and S4C); this peptide was not detectable in the presence of a reducing agent. Consistently, we observed the non-disulfide bonded peptide fragments in the presence of DTT (Figure4D). This peptide was ~100 fold enriched in the presence of DTT than in its absence (Table S1). This proved that the intermediate was trapped with an intramolecular-disulfide while refolding spontaneously in non-reducing conditions. Non-reducing gel electrophoresis confirmed that intermolecular disulfide is not a major species when refolding was initiated in the absence of DTT (Figure4E). This indicated that an intramolecular-disulfide rather than an intermolecular one traps the folding intermediate in a non-native state. Thus, the most likely model for spontaneous refolding of sGFP is through a refolding intermediate I_1 that is free to fold to its native state with an apparent rate of ~5e-3 s^{-1}. In oxidizing conditions, I_1 converts to a quasi-stable species with non-native contacts (I_1*) which rapidly converts to the intramolecular-disulfide bonded misfolded species (I_2) (Figure 4F, and S4D).

GroEL/ES accelerates refolding rate by decreasing entropic barrier

Since sGFP folds poorly in the absence of DTT, we asked if delayed addition of DTT could rescue the disulfide trapped refolding intermediate I_2. When the refolding was initiated in the presence of 2 µM $CuCl_2$(a catalyst of disulfide formation), delayed addition of DTT could not restore the sGFP

folding (Figure 5A), suggesting that sGFP in the disulfide-bonded state enters an irreversibly misfolded state I_2 that is refractile to reducing agents. Since more than 95% of the molecules reached I_2 within 5 minutes of the start of the refolding reaction, it shows that there is a rapid equilibrium between I_1 and I_1* (Figure 4F, dotted arrows) that is much faster than the time scale of folding. This suggested that the formation of I_1* did not affect the apparent rate of folding from I_1 to N.

Additionally, in conditions that favor disulfide formation, sGFP folding is limited by an enthalpic trap that is driven by non-native contact formation in the regions surrounding the two cysteines. The traps for this substrate could be switched on/off: the enthalpic trap could be switched off by DTT (reducing agent), and the entropic trap could be attenuated in the presence of salts.

Could the enthalpic traps generated by formation of non-native contacts be also rescued by GroEL/ES? Notably, the GroEL/ES system was able to accelerate the folding of sGFP and increase the yield of refolding even in the absence of DTT (Figure 5B). Since the cysteines are not proximal in the native structure, disulfide formation is dependent on non-native contact formation and hence misfolding. This suggested that GroEL/ES prevents the formation of a non-native contact during the conversion from I_1 to I_2. We performed a delayed addition experiment in which we delayed the addition of GroEL/ES system after initiating refolding of sGFP in the presence of 2 µM $CuCl_2$ (Figure 5C). Delayed addition of GroEL/ES led to a near complete loss of refolding indicating that GroEL/ES system was unable to break a preformed disulfide, as expected, and could only prevent the formation of a non-native disulfide by altering the folding path (Figure 5D). Taken together, the refolding intermediate (I_1) formed non-native contacts to form a quasi-stable species (I_1*) that rapidly formed non-native disulfide (under oxidizing conditions) to form the intermediate I_2. This intermediate is terminally misfolded and is refractile to folding assistance by DTT or GroEL/ES system. It appears that GroEL/ES system was able to prevent the formation of non-native contacts in I_1 (Figure 5D, red box) and hence the formation of I_2, channeling folding of sGFP through a productive route.

GroEL-binding is known to cause partial unfolding of proteins, and can potentially remove non-native interactions (Mapa et al., 2012; Sharma et al., 2008). To check this, we initiated refolding of sGFP in the presence of GroEL in a non-reducing buffer, but in the absence of GroES or ATP. GroEL alone did not assist refolding (Figure S5A). Delayed addition of GroES/ATP restarted refolding with the same rate as observed when GroEL/ES/ATP is added without any delay (Figure S5B). In contrast to delayed addition of the full GroEL/ES/ATP system, presence of GroEL prevented misfolding and the amplitude of refolding did not drop even after a 20 minute of delay

in adding GroES/ATP to GroEL-bound unfolded sGFP. (Figure 5E, and S5C). This proved that GroEL-binding to the non-native state of sGFP prevents the protein from forming non-native interactions, thereby maintaining it in a folding-competent state for a long time. Taken together, the GroEL/ES system or GroEL alone can prevent the cysteines from coming in close contact; thereby preventing the formation of non-native contacts that would result in enthalpic traps during folding.

While GroEL/ES was able to prevent I_1 to I_2 conversion, the refolding rate of GroEL/ES assisted folding was same in the presence or absence of DTT in the refolding reaction (Figure 5F). Essentially, GroEL/ES assisted refolding rate was faster than the spontaneous folding rate of sGFP even in the presence of DTT (Figure 5G). The refolding rate of sGFP did not increase as a function of DTT concentrations in the range used for the refolding here (Figure S5D) negating the argument that partial reduction of disulfide was the reason for slower folding than with GroEL/ES system. This clearly demonstrated that the GroEL/ES system can accelerate the refolding rate of sGFP even under (reducing) conditions where I_1 to I_2 conversion is completely prevented. Thus, in addition to preventing I_1 to I_2 conversion, GroEL/ES assistance increased the folding rate from I_1 to N irrespective of the redox condition of the refolding reaction (Figure 5D).

However, the enthalpic trap is not specific to K45E mutation of GFP, it is the property of the GFP backbone that shows redox dependent refolding amplitude and rate (Figure S5E). Thus, the entropic component of the folding barrier possibly renders the K45E mutation amenable to GroEL/ES dependent folding *in vivo* and *in vitro*.

Collectively, GroEL/ES works in a bipartite manner to assist sGFP refolding (Figure 3C, lower panel), 1) It prevents non-native contact formation and hence formation of non-productive off-pathway intermediates that have a strong potential to form a terminally misfolded conformation and 2) it decreases the entropic barrier in the folding pathway to increase the folding rate.

Implications

While proteins evolve, they accumulate mutations. A subset of these mutations may enhance the existing activity or impart new functions, they are also more likely to destabilize proteins than mutations on other regions of the protein surface (Tokuriki, Stricher, Serrano, & Tawfik, 2008). Chaperones have been proposed to aid these transitional sequences to allow them to cross barriers in fitness.

Aiming to link the molecular mechanism of chaperone-dependent buffering to the specific perturbations in protein-folding landscapes we used GroEL/ES as the model chaperone. We

found that GroEL/ES system buffers the entropic traps that can arise due mutations that stabilize the folding intermediates entropically.

Interestingly, GroEL/ES also had the capability to prevent formation of incorrect contacts in the folding polypeptide (rescue of enthalpic traps). However, this was not an exclusive activity of GroEL/ES as we show that even the DnaK/DnaJ/GrpE chaperone machinery also share this capability. Given that binding of non-native proteins with DnaK (Mapa et al., 2012; Mattoo et al., 2014or DnaJ {Tiwari, 2013 #1870; Rüdiger et al., 1997) or GroEL (Lin, Madan, & Rye, 2008; Sharma et al., 2008) can unfold protein chains and melt preformed contacts, it is conceivable that the holdase and the unfoldase action is required for removing enthalpic traps from folding landscapes. DnaK machinery in E. coli cytosol is more abundant than the GroEL/ES machinery and hence it is likely that mutations that introduce enthalpic traps in folding is more likely to be channeled through the former for efficient rescue.

While the current knowledge can be used in protein redesigning, our proposition, that GroEL/ES may specifically buffer mutations that traps flexible folding intermediates in entropic traps, will have interesting implications if it is found to be generally true in natural evolution.

METHODS

EXPERIMENTAL MODEL AND SUBJECT DETAILS

Strains, Plasmids and Proteins

E. coli strain DH5α was used for cloning, WT *E. coli* K-12 (BW25113) strain was used for expression of arabinose inducible pBAD GFP and BL21 (DE3) was used for protein expression and purification. Protein concentrations were determined spectrophotometrically at 562 nm using BCA kit (Pierce-ThermoFisher Scientific). Deletion strains were obtained from CGSC as part of Keio collection (Baba et al., 2006).

METHOD DETAILS

Construction of mutant GFP library

Mutant GFP library was made in arabinose inducible pBAD vector using random mutagenesis approach by error prone polymerase Mutazyme II that incorporated 7 to 11 mutations per kb of template. The said library has a total complexity of around 10,000 mutants. The reporter is constructed such that GFP and mCherry are under same arabinose inducible pBAD promoter in an operon to give readout of GFP according to the mutation created on it but the mCherry readout will remain similar thus serving as an internal control for transcription, translation and inducibility.

Screening of mutant GFP library for GroEL/ES dependent GFP mutant

Wild type *E.coli* cells (WT) were transformed with mutant GFP library maintaining 10-fold converge for preserving complexity. 0.4 OD600 cells were induced with 0.1% arabinose and fluorescence was observed three hours post induction at 37°C after diluting cells in 1X PBS and incubating at 37°C for further 1 hour. Fluorescence of the mutant library was studied in a pooled manner against wild type GFP. The entire library was sorted into populations of very low fluorescent, low fluorescent and mildly less fluorescent according to the GFP fluorescence. Each of these populations were purified and plasmids prepared. WT cells were co-transformed with GroEL/ES over-expressing plasmid (Castanie, Berges, Oreglia, Prere, & Fayet, 1997) and pool of GFP mutant plasmids in a sequential manner, maintaining the minimum 10X coverage. Pool of transformants were grown and GroEL/ES induced by adding 0.5 mM IPTG 30 minutes prior to induction of GFP by 0.1% arabinose. FACS was performed to sort *E.coli* cells showing high fluorescence upon GroEL/ES over expression. To confirm the dependence of sorted clones on GroEL/ES, plasmid pool was prepared from the sorted cells (harboring pBAD GFP as well as pOFX GroEL/ES) and digested using SacII (linearlizes pOFX GroEL/ES only) to obtain GFP clones post transformation in wild type *E.coli* cells. Single clones of GFP were picked from here and checked for their fluorescence in presence and absence of GroEL/ES overexpression. The isolated mutant having higher fluorescence in GroEL/ES overexpression was identified by Sanger sequencing. Isolated GroEL/ES dependent mutant of GFP (K45E) was cloned in pET SUMO between BamHI and HindIII restriction sites and purified using E. coli BL21 (DE3) for further characterization.

***E.coli* GroEL/ES, DnaK, DnaJ, GrpE Expression and Purification**

GroEL/ES, GroEL chimeras, DnaK, DnaJ, GrpE were purified using *E. coli* BL21 (DE3) as described (Kerner et al., 2005; Mapa et al., 2012; Tiwari, Kumar, Jayaraj, Maiti, & Mapa, 2013). GroEL/ES was expressed from pOFX plasmid for co-expression studies (Castanie et al., 1997).

Solubility of sGFP *in vivo*

WT *E.coli* cells containing pBAD sGFP were transformed with pOFX GroEL/ES. 0.1% inoculation was done in 10 ml LB medium added with chloramphenicol (35 µg/ml) from overnight grown cultures and grown till OD600-0.5 at 37°C, 200 rpm. 0.5 mM IPTG was added to cells with pOFX GroEL/ES 30 minutes before induction of sGFP with 0.1% arabinose for 3 hours. The cell type in which we transformed only pBAD sGFP were directly induced with 0.1% arabinose for 3 hours after reaching OD600- 0.5. Cells were harvested at 4000 rpm for 10 minutes and resuspended in 1 ml PBS pH 7.4, 2 mM DTT. Lysis was done using sonication followed by high speed centrifugation to separate soluble and pellet fraction which were separately loaded onto 12% SDS-PAGE. Gel visualized by Coomassie staining.

Spontaneous and chaperonin assisted *in vitro* refolding of sGFP

Wt GFP and sGFP (20 µM each) were denatured in buffer containing 6 M GuHCl in buffer A (20 mM Tris, 20 mM KCl, 5 mM $MgCl_2$, 2 mM DTT, pH 7.4) for 1 hour at 25°C and refolded upon 100 fold dilution into buffer A. Either of three refolding buffers were used for refolding, buffer A to mimic reducing conditions, buffer B (20 mM Tris, 20 mM KCl, 5 mM $MgCl_2$, pH 7.4) to mimic non-reducing conditions and buffer C (20 mM Tris, 20 mM KCl, 5 mM $MgCl_2$, 2 µM $CuCl_2$, pH 7.4) to mimic oxidizing conditions.

GroEL/ES assisted refolding was done in the presence of (400 nM) GroEL (tetradecamer), (800 nM) GroES (heptamer), (substrate:GroEL:ES :: 1:2:4) and the refolding was started by addition of 2 mM ATP. SR-EL/ES assisted refolding was done in presence of (800 nM) of SR-EL (heptamer) (800 nM) GroES (heptamer) and the refolding was started by addition of 2 mM ATP. GFP fluorescence at 480 nm excitation (slit width 2 nm) and 515 nm emission (10 nm slit width) was monitored as a read out of refolding using Fluorolog 3 Spectrofluorometer (Horiba). Buffer conditions are described in the figures. All the unfolding and refolding experiments were carried out at 25°C unless specified.

GuHCl concentration dependent spontaneous and chaperonin assisted *in vitro* refolding of sGFP

sGFP (80µM) were denatured in buffer containing 6 M GuHCl in buffer A for 1 hour at 25°C and was refolded upon 400 times dilution in buffer A alone or buffer A containing (400 nM) GroEL (tetradecamer), (800 nM) GroES (heptamer) and the refolding was started by addition of 2 mM ATP. GuHCl present in unfolded sGFP was diluted to 15 mM upon 400 times dilution in buffer A. GuHCl concentration was increased to 30 mM, 45 mM, 60 mM by adding GuHCl from outside in refolding mixture.

Analysis of temperature dependent refolding using Arrhenius equation

In order to obtain thermodynamic parameters that define the barrier between the refolding intermediate I_1 and the transition state (TS) of folding we used the following equation essentially as defined in (Dandage et al., 2015).

$$k_f = \rho\, T e^{-\frac{\Delta H^{\#} - \Delta C_p^{\#}\left(T - T_0 - T ln\left(\frac{T}{T_0}\right)\right)}{RT}}$$

Where

$$\rho = \left(\frac{k_B}{h}\right)\left(\kappa . e^{\frac{\Delta S^{\#}}{R}}\right)$$

and k_f is refolding rate, R is the universal gas constant, $\Delta H^{\#}$, $\Delta S^{\#}$ and $\Delta C_p^{\#}$ are the differences in enthalpy, entropy and heat capacity at constant pressure and the reference temperature T_0 between TS and I_1, respectively, T is the temperature of refolding reaction, T_0 is the reference temperature at which the parameters are determined (here it is 298.15 K). κ is the transmission factor, that reports the proportion of activations that lead to the formation of the native state (N), and k_B and h are Boltzmann and Planck constant respectively. Since $\Delta S^{\#}$ and A linearly combine, it is not possible to obtain independent estimates of these two parameters by non-linear regression. Hence, we combine it to obtain ρ. This term indicates the ease of barrier crossing, either because the diffusion is faster or because the barrier is less broad (due to lower $\Delta S^{\#}$). A high $\Delta H^{\#}$ indicate higher barrier, and a low ρ indicates an entropic (diffusion-limited) barrier. The equations were fitted using standard non-linear regression fitting using R or Octave.

Mass spectrometry analysis for disulfide bond detection:

5µg of control or DTT treated sGFP was digested by using sequencing grade trypsin (1:10 ratio, Trypsin:protein) for 16-18 hours at 37°C. Before digestion DTT treated sample was alkylated by using 55 mM iodoacetamide. Tryptic digested peptides were reconstituted in 5µl of LC-MS grade water containing 0.1% formic acid and run on a quadrupole-TOF hybrid mass spectrometer (TripleTOF 6600, Sciex, USA) coupled to a nano-LC system (Eksigent NanoLC-400). Two microliters of sample was injected and loaded onto a reverse phase peptide ChromoLC trap (200 mm 0.5 mm) column and peptides were separated using a C18 column (75 mm 15 cm, Eksigent). The samples were run using a gradient method using buffer X (99.9% LC-MS water + 0.1% formic acid) and buffer Y (99.9% acetonitrile + 0.1% formic acid). The gradient consists of 95% of buffer X for 2 minutes, and then shifted to 90% of buffer X for 8 minutes, and then decreased to 20% of

buffer X in 42 minutes and finally shifted to 95% of buffer X again for 16 minutes at a consistent flow rate of 250 nl min-1. Data was acquired with a NanoSpray source installed in the TripleTOF 6600 System using a nebulizing gas of 20 psi, a curtain gas of 25 psi, an ion spray voltage of 2000 V and a heater interface temperature of 75 0C. Information-dependent acquisition (IDA) mode was setup with a TOF/MS survey scan (350–1600 m/z) with an accumulation time of 250 ms. For fragmentation a maximum of ten precursor ions per cycle were selected with each MS/MS spectrum (200–1800 m/z) accumulated for 70 ms with a total cycle time of approximately 2.05 seconds. Parent ions with a charge state from +2 to +5 and abundance of more than 150 cps were selected for MS/MS fragmentation. Once an ion had been fragmented by MS/MS, its mass and isotopes were excluded for a period of 3 seconds. The wiff files generated from Triple TOF 6600 (which contain both MS and MS/MS spectra) were analyzed using the protein pilot v5.0 for identification of our desire protein. For disulfide bond detection and further spectra analysis was done using Biopharma view v2.0 and peak view 2.2 software (Sciex).

QUANTIFICATION AND STATISTICAL ANALYSIS

Student t-test and R package for non-linear regression was used for statistical analysis. Flow-cytometry data was analyzed using octave.

DATA AND SOFTWARE AVAILABILITY

All data are provided in the manuscript. We did not develop any new software.

KEY RESOURCE TABLE

REAGENT or RESOURCE	SOURCE	IDENTIFIER
Antibodies		
Rabbit anti GFP	Abcam	AB290
Bacterial and Virus Strains		

E.coli BL21 (DE3)		
E.coli DH5α		
E.coli WT (K-12, BW25113) F-, DE(araD-araB)567, lacZ4787(del)::rrnB-3, LAM-, rph-1, DE(rhaD-rhaB)568, hsdR514	(Baba et al., 2006)	CGSC#: 7636
∆*Tig* (JW0426-1) *F-, Δ(araD-araB)567, ΔlacZ4787(::rrnB-3), Δtig-722::kan, λ-, rph-1, Δ(rhaD-rhaB)568, hsdR514*	(Baba et al., 2006)	CGSC#: 8589
∆*dnaK (*JW0013-4) F-, Δ(araD-araB)567, ΔlacZ4787(::rrnB-3), λ-, rph-1, ΔdnaK734::kan, Δ(rhaD-rhaB)568, hsdR514	(Baba et al., 2006)	CGSC#: 8342
∆*dnaJ (*JW0014-1) F-, Δ(araD-araB)567, ΔlacZ4787(::rrnB-3), λ-,rph-1, ΔdnaJ735::kan,Δ(rhaD-rhaB)568, hsdR514	(Baba et al., 2006)	CGSC#: 8343
Chemicals, Peptides, and Recombinant Proteins		
Proteinase K	MP Biomedicals	Cat#193981
ATP	Sigma	Cat#A2383
Oligonucleotides		
yeGFP Forward primer: CCCGGATCCATGTCTAAAGGTGAAGAATTATTCACTGGTGTTGTCCC	This Paper	
yeGFP Reverse primer: CCCAAGCTTTTATTTGTACAATTCATCCATACCATGGGTAATA	This Paper	
Recombinant DNA		

pOFX ELES (pOFX tac-SL2)	(Castanie et al., 1997)	
pOFX DnaK/J/GrpE (pOFX tac-KJE1)	(Castanie et al., 1997)	
pET duet1 dnaK	(Tiwari et al., 2013)	
pET duet1 dnaJ	(Tiwari et al., 2013)	
pET duet1 grpE	(Tiwari et al., 2013)	
pET SUMO sGFP	This Paper	
Software and Algorithms		
Chimera		
ABPS		

ACKNOWLEDGEMENT

We thank Kanika Saxena for sharing the starting plasmid with GFP and mCherry. The work was done in KM Lab with the grant YSS/2015/000532 from SERB India, and partly from SNU core funding. The work in KC Lab was supported by Swarnajayanthi Fellowship Grant from DST, and partly from BSC0124 from CSIR. Instrument support was also obtained from Wellcome Trust-DBT India Alliance and CSIR. KM, MA acknowledge SNU, and KC acknowledges CSIR and CSIR-IGIB for infrastructural support. A. Sadat and ST acknowledges DBT; AR, KV, AC, A. Singh acknowledge CSIR; RC acknowledge UGC for fellowship support.

AUTHOR CONTRIBUTION

Conceptualization: Koyeli Mapa

Supervision: Koyeli Mapa, Kausik Chakraborty

Reagent Generation: Satyam Tiwari, Kanika Verma, Anwar Sadat, Aseem Chaphalkar,

Experiments: Anwar Sadat, Satyam Tiwari, Kanika Verma, Mudassar Ali, Vaibhav Upadhyay, Anupam Singh, Aseem Chaphalkar, Rahul Chakraborty, Kausik Chakraborty

Analysis: Arjun Ray (computational), Anwar Sadat (biophysics), Satyam Tiwari (biophysics), Kanika Verma (FACS), Rahul Chakraborty (MS), Kausik Chakraborty, Koyeli Mapa

Manuscript writing: Koyeli Mapa and Kausik Chakraborty with inputs from Anwar Sadat, Kanika Verma, and Aseem Chaphalkar. All the authors read and edited the manuscript.

DECLARATIONS OF INTEREST

The authors declare no competing interests.

References

Baba, T., Ara, T., Hasegawa, M., Takai, Y., Okumura, Y., Baba, M., . . . Mori, H. (2006). Construction of Escherichia coli K-12 in-frame, single-gene knockout mutants: the Keio collection. *Mol Syst Biol, 2*, 2006 0008. doi: 10.1038/msb4100050

Bandyopadhyay, B., Goldenzweig, A., Unger, T., Adato, O., Fleishman, S. J., Unger, R., & Horovitz, A. (2017). Local energetic frustration affects the dependence of green fluorescent protein folding on the chaperonin GroEL. *J Biol Chem, 292*(50), 20583-20591. doi: 10.1074/jbc.M117.808576

Calloni, G., Chen, T., Schermann, S. M., Chang, H. C., Genevaux, P., Agostini, F., . . . Hartl, F. U. (2012). DnaK functions as a central hub in the E. coli chaperone network. *Cell Rep, 1*(3), 251-264. doi: 10.1016/j.celrep.2011.12.007

Castanie, M. P., Berges, H., Oreglia, J., Prere, M. F., & Fayet, O. (1997). A set of pBR322-compatible plasmids allowing the testing of chaperone-assisted folding of proteins overexpressed in Escherichia coli. *Anal Biochem, 254*(1), 150-152. doi: 10.1006/abio.1997.2423

Chakraborty, K., Chatila, M., Sinha, J., Shi, Q., Poschner, B. C., Sikor, M., . . . Hayer-Hartl, M. (2010). Chaperonin-catalyzed rescue of kinetically trapped states in protein folding. *Cell, 142*(1), 112-122. doi: 10.1016/j.cell.2010.05.027

Chiti, F., & Dobson, C. M. (2017). Protein Misfolding, Amyloid Formation, and Human Disease: A Summary of Progress Over the Last Decade. *Annu Rev Biochem, 86*, 27-68. doi: 10.1146/annurev-biochem-061516-045115

Dandage, R., Bandyopadhyay, A., Jayaraj, G. G., Saxena, K., Dalal, V., Das, A., & Chakraborty, K. (2015). Classification of chemical chaperones based on their effect on protein folding landscapes. *ACS Chem Biol, 10*(3), 813-820. doi: 10.1021/cb500798y

Dunn, A. Y., Melville, M. W., & Frydman, J. (2001). Review: cellular substrates of the eukaryotic chaperonin TRiC/CCT. *J Struct Biol, 135*(2), 176-184. doi: 10.1006/jsbi.2001.4380

Georgescauld, F., Popova, K., Gupta, A. J., Bracher, A., Engen, J. R., Hayer-Hartl, M., & Hartl, F. U. (2014). GroEL/ES chaperonin modulates the mechanism and accelerates the rate of TIM-barrel domain folding. *Cell, 157*(4), 922-934. doi: 10.1016/j.cell.2014.03.038

Hartl, F. U. (2017). Protein Misfolding Diseases. *Annu Rev Biochem, 86*, 21-26. doi: 10.1146/annurev-biochem-061516-044518

Horwich, A. L., Burston, S. G., Rye, H. S., Weissman, J. S., & Fenton, W. A. (1998). [11] Construction of single-ring and two-ring hybrid versions of bacterial chaperonin GroEL *Methods in enzymology* (Vol. 290, pp. 141-146): Elsevier.

Houry, W. A., Frishman, D., Eckerskorn, C., Lottspeich, F., & Hartl, F. U. (1999). Identification of in vivo substrates of the chaperonin GroEL. *Nature, 402*(6758), 147-154. doi: 10.1038/45977

Kerner, M. J., Naylor, D. J., Ishihama, Y., Maier, T., Chang, H. C., Stines, A. P., . . . Hartl, F. U. (2005). Proteome-wide analysis of chaperonin-dependent protein folding in Escherichia coli. *Cell, 122*(2), 209-220. doi: 10.1016/j.cell.2005.05.028

Knoblauch, N. T., Rüdiger, S., Schönfeld, H. J., Driessen, A. J., Schneider-Mergener, J., & Bukau, B. (1999). Substrate specificity of the SecB chaperone. *J Biol Chem, 274*(48), 34219-34225. doi: 10.1074/jbc.274.48.34219

Lin, Z., Madan, D., & Rye, H. S. (2008). GroEL stimulates protein folding through forced unfolding. *Nat Struct Mol Biol, 15*(3), 303-311. doi: 10.1038/nsmb.1394

Mapa, K., Tiwari, S., Kumar, V., Jayaraj, G. G., & Maiti, S. (2012). Information encoded in non-native states drives substrate-chaperone pairing. *Structure, 20*(9), 1562-1573. doi: 10.1016/j.str.2012.06.014

Mattoo, R. U., Farina Henriquez Cuendet, A., Subanna, S., Finka, A., Priya, S., Sharma, S. K., & Goloubinoff, P. (2014). Synergism between a foldase and an unfoldase: reciprocal dependence between the thioredoxin-like activity of DnaJ and the polypeptide-unfolding activity of DnaK. *Front Mol Biosci, 1*, 7. doi: 10.3389/fmolb.2014.00007

Nagpal, S., Tiwari, S., Mapa, K., & Thukral, L. (2015). Decoding Structural Properties of a Partially Unfolded Protein Substrate: En Route to Chaperone Binding. *PLoS Comput Biol, 11*(9), e1004496. doi: 10.1371/journal.pcbi.1004496

Niwa, T., Fujiwara, K., & Taguchi, H. (2016). Identification of novel in vivo obligate GroEL/ES substrates based on data from a cell-free proteomics approach. *FEBS Lett, 590*(2), 251-257. doi: 10.1002/1873-3468.12036

Pettersen, E. F., Goddard, T. D., Huang, C. C., Couch, G. S., Greenblatt, D. M., Meng, E. C., & Ferrin, T. E. (2004). UCSF Chimera--a visualization system for exploratory research and analysis. *J Comput Chem, 25*(13), 1605-1612. doi: 10.1002/jcc.20084

Rüdiger, S., Germeroth, L., Schneider-Mergener, J., & Bukau, B. (1997). Substrate specificity of the DnaK chaperone determined by screening cellulose-bound peptide libraries. *Embo j, 16*(7), 1501-1507. doi: 10.1093/emboj/16.7.1501

Sharma, S., Chakraborty, K., Muller, B. K., Astola, N., Tang, Y. C., Lamb, D. C., . . . Hartl, F. U. (2008). Monitoring protein conformation along the pathway of chaperonin-assisted folding. *Cell, 133*(1), 142-153. doi: 10.1016/j.cell.2008.01.048

Tiwari, S., Kumar, V., Jayaraj, G. G., Maiti, S., & Mapa, K. (2013). Unique structural modulation of a non-native substrate by cochaperone DnaJ. *Biochemistry, 52*(6), 1011-1018. doi: 10.1021/bi301543g

Tokuriki, N., Stricher, F., Serrano, L., & Tawfik, D. S. (2008). How protein stability and new functions trade off. *PLoS Comput Biol, 4*(2), e1000002. doi: 10.1371/journal.pcbi.1000002

Verma, K., Saxena, K., Donaka, R., Chaphalkar, A., Rai, M. K., Shukla, A., . . . Chakraborty, K. (2019). Distinct metabolic states of a cell guide alternate fates of mutational buffering through altered proteostasis. *bioRxiv*, 540039.

Xu, Z., Horwich, A. L., & Sigler, P. B. (1997). The crystal structure of the asymmetric GroEL-GroES-(ADP)7 chaperonin complex. *Nature, 388*(6644), 741-750. doi: 10.1038/41944

Yang, F., Moss, L. G., & Phillips, G. N., Jr. (1996). The molecular structure of green fluorescent protein. *Nat Biotechnol, 14*(10), 1246-1251. doi: 10.1038/nbt1096-1246

Zhao, L., Vecchi, G., Vendruscolo, M., Körner, R., Hayer-Hartl, M., & Hartl, F. U. (2019). The Hsp70 Chaperone System Stabilizes a Thermo-sensitive Subproteome in E. coli. *Cell Rep, 28*(5), 1335-1345.e1336. doi: 10.1016/j.celrep.2019.06.081

FIGURE LEGENDS:

Figure 1: Laboratory evolution of an authentic substrate of GroEL/ES

(A) Upper panel: Histogram for *in vivo* fluorescence of Wt GFP (represented as the ratio of GFP/mCherry) in presence and absence of plasmid-based overexpression of GroEL/ES.

Lower panel: Refolding kinetics of Wt GFP in the presence and absence of GroEL/ES/ATP. Spontaneous refolding of Wt GFP was initiated by a 100-fold dilution of the unfolded proteins in buffer A (20 mM Tris, 20 mM KCl, 5 mM $MgCl_2$, 2 mM DTT, pH 7.4) at 25˚C. For GroEL/ES assisted refolding unfolded protein was diluted 100-fold in buffer A containing 400 nM of GroEL (all concentrations of GroEL are in terms of tetradecamer), 800 nM GroES (all concentration of GroES are in terms of heptamer) so that the final concentration of unfolded protein is 200 nM. Subsequently, refolding was initiated by adding 2 mM ATP. Recovery of GFP fluorescence over time was followed to monitor refolding.

(B) Schematic of the bicistronic construct of GFP and mCherry drove by an Arabinose inducible system. RBS indicates the position of the additional ribosome binding site (RBS) to initiate translation of mCherry.

(C) Upper panel: Scatter plot of *E. coli* WT cells expressing random mutant library of GFP. Red box highlights population of cells with low GFP fluorescence (LF-GFP) compared to Wt GFP, with same mCherry fluorescence as that of Wt GFP.

Lower panel: Histogram for flow cytometry of cells harboring low-fluorescent (LF) mutant pool of GFP and the Wt GFP. GFP/mCherry ratio is monitored at a single cell level.

(D) Upper panel: Schematic of FACS to isolate GroEL/ES-dependent mutant GFP clones.

Lower panel: The cells harboring LF-GFP library were induced to express GFP mutants either alone or along with the GroEL/ES system. Negative gating (gate I) was defined by the single-cell GFP/mCherry ratio of the LF-GFP when expressed alone (red dots). Separately, LF-GFP expression was induced in the presence of overexpressed GroEL/ES (blue dots), Positive clones were sorted by gating for cells that had higher GFP/mCherry ratio than Gate I (Postive gate). Gate I included cells only with high GFP fluorescence along with high GFP/mCherry ratio.

(E) K45 residue depicted on the crystal structure of GFP (1GFL (Xu, Horwich, & Sigler, 1997; Yang, Moss, & Phillips, 1996)) showing its surface exposure away from the buried fluorophore. Some of the residues in beta-sheets facing the viewer are not shown in order to make the fluorophore underneath clearly visible. Only one chain of GFP is shown for clarity. Depiction made using Chimera (Pettersen et al., 2004).

(F) Histogram of single-cell GFP/mCherry ratio of sGFP (GFP (K45E)) in the presence and absence of GroEL/ES over-expression. For individual histogram of GFP and mCherry please see Figure S1C.

(G) *in vivo* solubility of sGFP in the absence (left panel) and presence (right panel) of GroEL/ES over-expression. Partitioning of sGFP is shown in the total lysate (T), pellet fraction (P) and soluble fraction (S).

See Figure S1.

Figure 2: A comprehensive folding landscape for sGFP

(A) Comparison of the refolding rate of WtGFP and sGFP. WtGFP and sGFP were unfolded in 6 M GuHCl in buffer A for 1 hour at 25°C. Refolding was initiated by a 100-fold dilution of the unfolded proteins in buffer A (20 mM Tris, 20 mM KCl, 5 mM $MgCl_2$, 2 mM DTT, pH 7.4) at 25°C so that the final concentration of the proteins was 200 nM. Refolding was monitored by following the fluorescence of GFP with time.

(B) Refolding rate and amplitude as a function of sGFP concentration. sGFP was unfolded as described earlier but at different concentration. Refolding was initiated from each of these by a 100-fold dilution into buffer A such that the final protein concentrations were 12.5, 100, 200, or

400 nM. Refolding was monitored by measuring the recovery of GFP fluorescence over time. The refolding traces were fitted to obtain the apparent folding rate (red circles) and the percentage of expected amplitude (black circles). These were plotted as a function of protein concentration. Expected amplitude was calculated based on the fluorescence recovery upon refolding protein at 400 nM concentration.

(C) Arrhenius plot for sGFP and Wt GFP refolding. Refolding of sGFP or Wt GFP was initiated as described earlier. The refolding reactions were initiated in buffer A that were preincubated at different temperatures (15°C, 20°C, 25°C, 30°C and 35°C) and monitored by measuring the recovery of GFP fluorescence. Rates obtained by fitting the refolding traces obtained at different temperatures are plotted against (1/T) for sGFP (grey circles), and Wt GFP (black circles). The rates were obtained from independent replicates of 3 refolding reactions at each temperature. Line plots are the fits obtained by fitting the temperature dependent refolding rates to the Arrhenius equation as described in the supplemental text.

(D) The calculated enthalpy of activation (ΔH#), and ρ obtained from Arrhenius fitting of sGFP and Wt GFP refolding shown in (C).

(E) Close up of K45 (orange - side chain carbons of K45, navy blue - εN) region on GFP (using 1GFL), and its interacting amino acids. The model was prepared using Chimera.

(F) Comparison of the refolding rate of sGFP in the presence of different salts of equal ionic strength. Spontaneous refolding of sGFP was initiated by a 100-fold dilution of the unfolded proteins in buffer A at 25°C. For salt assisted refolding unfolded protein was diluted 100-fold in buffer A containing of different salts (100 mM $MgCl_2$, or 300 mM NaCl, or 300 mM KCl) of equal ionic strength so that the final concentration of unfolded protein is 200 nM. Recovery of GFP fluorescence over time was followed to monitor refolding.

See Figure S2 and S3.

Figure 3: GroEL/ES alters the folding pathway of sGFP

(A) Left panel: Comparison of the refolding rate of sGFP in the presence and absence of GroEL/ES/ATP. Spontaneous refolding of sGFP was initiated as mentioned earlier either in buffer A. For GroEL/ES assisted refolding unfolded protein was diluted 100-fold in buffer A containing 400 nM of GroEL (all concentrations of GroEL are in terms of tetradecamer), 800 nM GroES (all the concentrations of GroES are in terms of heptamer) so that the final concentration of unfolded

protein is 200 nM. Subsequently, refolding was started by adding 2 mM ATP. Recovery of GFP fluorescence over time was followed to monitor refolding.

Right panel: Refolding traces were fitted to single exponential kinetics to obtain the refolding rates shown as bar plots. Three independent refolding runs were fitted separately to obtain the standard deviation in rates (shown as errors on the bar graph).

(B) Monitoring the dependence of sGFP refolding on the different components of EL/ES. Unfolded sGFP was diluted 100-fold either in the presence of GroEL (400 nM), or GroEL (400 nM) + GroES (800 nM) or GroEL (400 nM) + ATP (2 mM) or GroEL (400 nM) + GroES (800 nM) + ATP (2 mM) and refolding was monitored by the recovery of GFP fluorescence.

(C) The calculated enthalpy of activation ($\Delta H^{\#}$), and ρ obtained from Arrhenius fitting of GroEL/ES/ATP and SR-EL/ES/ATP assisted refolding of sGFP.

(D) Effect of GuHCl on refolding rate upon spontaneous and GroEL/ES/ATP assisted refolding of sGFP. The rates [$\ln(k_f)$] of spontaneous and GroEL/ES/ATP assisted refolding of sGFP at different GuHCl concentration are plotted against different GuHCl concentrations.

(E) The m-value (dependence of refolding rate on GuHCl concentration) of folding upon spontaneous, GroEL/ES/ATP and SR-EL/ES/ATP assisted refolding of sGFP.

Figure 4: GroEL/ES prevents non-native contact formation

(A) Refolding of sGFP was initiated in buffer A (shown as +DTT) or buffer B (20 mM Tris, 20 mM KCl, 5 mM $MgCl_2$, pH 7.4) (shown as -DTT). Refolding was monitored by the recovery of GFP fluorescence over time.

(B) Schematic representation of a hypothetical fragment pattern when an intramolecular disulfide is formed (in the absence of DTT) and in its absence (in the presence of DTT).

(C) The expected peptide sequence and mass upon the formation of the intramolecular disulfide is shown along with the experimentally observed isotopic mass distribution obtained for the peptide when refolding of sGFP is initiated in the absence of DTT.

(D) The peptide fragment expected when disulfide bonding is prevented during sGFP refolding in DTT, and the experimentally observed isotopic mass distribution for the peptide is shown.

(E) Non-reducing PAGE to monitor the formation of intermolecular disulfide bonds. Folding of sGFP was initiated as described earlier in buffer B or buffer A at a final concentration of 500 nM

sGFP. The proteins were then boiled and loaded onto a non-reducing polyacrylamide gel to resolve the proteins. Immunoblotting was performed to detect sGFP using anti-GFP antibody.

(F) A simplistic model of the spontaneously refolding sGFP. The unfolded state reaches the folding intermediate I_1 which then converts to the native state N. I_1 is in rapid equilibrium with I_1* where the cysteines (shown as orange circles) come in close proximity. I_1*, in turn, can form the disulfide in oxidizing conditions and form a terminally misfolded state I_2 that is refractile to refolding even in the presence of DTT.

See Figure S4.

Figure 5: GroEL/ES accelerates refolding rate by decreasing entropic barrier

(A) Effect of delayed addition of DTT to spontaneously refolding sGFP. sGFP refolding was initiated in buffer C (20 mM Tris, 20 mM KCl, 5 mM $MgCl_2$, 2 μM $CuCl_2$ pH 7.4) at a final concentration of 200 nM of sGFP. DTT was either added before unfolded sGFP was diluted in the buffer to start refolding (0 delay) or after 5 min or 10 min. Refolding traces for 5 min and 10 minutes delayed addition of DTT are shown from the time DTT was added.

(B) Spontaneous or GroEL/ES dependent refolding of sGFP was initiated as described earlier, except that the refolding was performed in buffer B for both the refolding reactions.

(C) Effect of delayed addition of GroEL/ES/ATP to spontaneously refolding sGFP. Refolding of sGFP was initiated as earlier in buffer C, and GroEL/ES/ATP (400 nM/800 nM/2 mM respectively) was added after a time-delay of 5 min or 10 min. For zero delay, GroEL/ES/ATP was added to buffer C before adding unfolded sGFP.

(D) Refolding pathway of sGFP in the presence and absence of GroEL/ES. GroEL/ES/ATP efficiently prevents the formation of I_1* (shown by the red arrow) and also allows more efficient conversion of I_1 to N (shown by the green arrow).

(E) GroEL-binding is sufficient to prevent sGFP misfolding. sGFP refolding was initiated as earlier, in buffer C containing 400 nM GroEL. GroES/ATP (800 nM/2 mM, respectively) was added after time delays of 5 min, 10 min or 20 min. Refolding was monitored although the time course, traces shown are after addition of GroES/ATP. For zero delay addition, GroES/ATP was present along with GroEL in buffer C before unfolded sGFP was added to the buffer.

(F) Effect of DTT on GroEL/ES assisted refolding rate of sGFP. (E) Refolding of sGFP was initiated as described in buffer C (black line), buffer C containing GroEL/ES/ATP (400 nM, 800

nM, 2 mM, respectively) (red line), buffer A (blue line), and buffer A containing GroEL/ES/ATP (400 nM, 800 nM, 2 mM, respectively) (maroon circles).

(G) Rates for refolding in the latter three (from Figure 5F) were obtained by fitting to exponential rate equation and is shown as bar graphs. Errors shown are standard deviations over three independent replicates.

See Figure S5.

Supplementary Figures:

Figure S1: related to Figure 1

(A) Bar graph for *in vivo* fluorescence of GroEL/ES dependent 10 single GFP clones isolated through FACS with (red) and without (black) GroEL/ES overexpression.

(B) Native fluorescence of sGFP (K45E) compared to Wt GFP.

(C) Independent fluorescence of GFP and mCherry channel for sGFP with (red) and without (black) GroEL/ES overexpression. GroEL/ES overexpression leads to an increase in GFP fluorescence (left panel) with similar mCherry fluorescence (right panel).

(D) Independent fluorescence of GFP and mCherry channel for sGFP with (red) and without (black) plasmid based DnaK/J/GrpE overexpression. Overexpression of DnaK/J/GrpE decreases GFP fluorescence (upper panel) with no effect on mCherry fluorescence (lower panel).

(E) Independent fluorescence of GFP (upper panel) and mCherry (lower panel) channel for sGFP in WT cells and in cells with single gene knockout of the most abundant chaperones (*Δtig*, *ΔdnaK*, and *ΔdnaJ*)

Figure S2: related to Figure 2

(A) sGFP was unfolded in 6 M GuHCl in buffer A for 1 hour at 25˚C. Unfolding was monitored by following the decrease in fluorescence of GFP with time.

(B) Refolding kinetics of spontaneously refolding sGFP in buffer A as followed by GFP fluorescence (upper panel open circles). Single exponential fit to the refolding is shown as red line in upper panel. The scatter from residuals are shown in the bottom panel.

(C-D) sGFP refolding kinetics as a function of its concentration (C). sGFP was unfolded as described earlier but at different concentration. Refolding was initiated from each of these by a 100-fold dilution into buffer A such that the final protein concentrations were 12.5, 100, 200, or 400 nM. Refolding was monitored by measuring the recovery of GFP fluorescence over time. The plot of normalized GFP fluorescence/time (D).

(E) Comparison of the refolding rate of sGFP (left panel) and Wt GFP (right panel) in the presence of different concentrations of $MgCl_2$. Spontaneous refolding of both the proteins was initiated by a 100-fold dilution of the unfolded proteins in buffer A at 25˚C containing different concentrations of $MgCl_2$ as shown in the figure. Recovery of GFP fluorescence over time was followed to monitor refolding.

Figure S3: Schematic showing barriers in the folding landscape, related to Figure 2

(A) A section of the folding funnel is represented in all cases. Unfolded state (U) forms the folding intermediate (I) that are separated by a transition state (TS) from the native state (N) of the protein. Inset shows the axis - vertical axis represents enthalpy, whereas the cylindrical axis (distance from the centre of rotation) represents entropy of the protein chain.
Upper panel schematically shows an enthalpic barrier in folding, essentially a hill in the enthalpy axis, that leads to slower folding. A decrease in the height of the hill (decreasing $\Delta H^{\#}$) leads to faster folding (right panel).
Lower panel schematically depicts an entropic barrier. The intermediate (I) is a flat area in the landscape that delays folding as the conformational search is undirected and it takes time to reach TS. The flatness is inversely proportional to ρ and hence a lower ρ indicates slow folding (left panel) while an increase in ρ (decrease in the flat basin) leads to accelerated folding (right panel).

(B) Refolding kinetics of sGFP in the presence and absence of DnaK/J/GrpE/ATP. Unfolded protein was diluted 100-fold in buffer A containing 800 nM of DnaK, 400 nM DnaJ, 800 nM GrpE (2:1:2), so that the final concentration of unfolded protein is 200 nM. Subsequently, refolding was initiated by adding 5 mM ATP. Recovery of GFP fluorescence over time was followed to monitor refolding.

Figure S4: related to Figure 4

(A) Refolding kinetics of sGFP in the presence and absence of $CuCl_2$. Spontaneous refolding of sGFP was initiated by a 100 fold dilution of the unfolded proteins in buffer B at 25˚C. For $CuCl_2$ assisted refolding unfolded protein was diluted 100-fold in buffer B containing 2μM of $CuCl_2$ so that the final concentration of unfolded protein is 200 nM. Recovery of GFP fluorescence over time was followed to monitor refolding.

(B) Figure showing the distance between C48 and C70 position (Cysteine 48 and 70 (orange), connecting line between two cysteines (red)) on native GFP (using 1GFL). The figure made using Chimera.

(C) Schematic showing the preparation of sample for LC-MS. sGFP was unfolded as described earlier and refolded by 100-fold dilution in buffer A and B for 30 minutes. Buffer exchange of sGFP was done in 500 mM TEAB buffer. Then sGFP was subjected to digestion by trypsin for 18 hours at 37˚C. The digested product was vacuum dried and run in LC-MS.

(D) Qualitative one-dimensional energy landscape for spontaneously refolding sGFP. Black denotes the energy landscape of sGFP while refolding in the presence of DTT. Red dashed line shows the change in the landscape in the presence of $CuCl_2$. Rest of the landscape remains unchanged.

Figure S5: related to Figure 5

(A) Comparison of the refolding kinetics of sGFP in the presence of different components of GroEL/ES/ATP. Spontaneous refolding of sGFP was initiated as mentioned earlier in buffer B at 25˚C. For different component of GroEL/ES/ATP assisted refolding unfolded protein was diluted 100-fold in buffer C containing either GroEL alone or GroEL/ATP or GroEL/ES/ATP so that the final concentration of unfolded protein is 200 nM. Recovery of GFP fluorescence over time was followed to monitor refolding.

(B) Comparison of the refolding rate of sGFP upon delayed addition of GroES/ATP to GroEL bound sGFP. Refolding of sGFP and was initiated as earlier in buffer C in the presence of GroEL, and GroES/ATP was added after a time-delay of 5, 10 or 20 minutes. For no delay, GroEL/ES/ATP was added to buffer C before adding unfolded sGFP.

(C) Refolding kinetics of sGFP upon delayed addition of GroES/ATP to GroEL bound sGFP (similar to figure S5B).

(D) Refolding rate as a function of DTT concentration. sGFP was unfolded as described earlier and refolding was initiated by a 100-fold dilution into buffer B containing different concentrations of DTT (2,3 and 4 mM) such that the final protein concentrations were 200 nM. Refolding was monitored by measuring the recovery of GFP fluorescence over time. Refolding traces were fitted to single exponential kinetics to obtain the refolding rates shown as bar plots with standard deviation in rates (shown as errors on bar graph).

(E) Effect of non-reducing (in buffer B, shown as - DTT) and reducing environment (in buffer A, shown as + DTT) on GFP backbone, in terms of refolding rate. Error bars indicate standard deviation from three independent replicates.

FIGURE 1

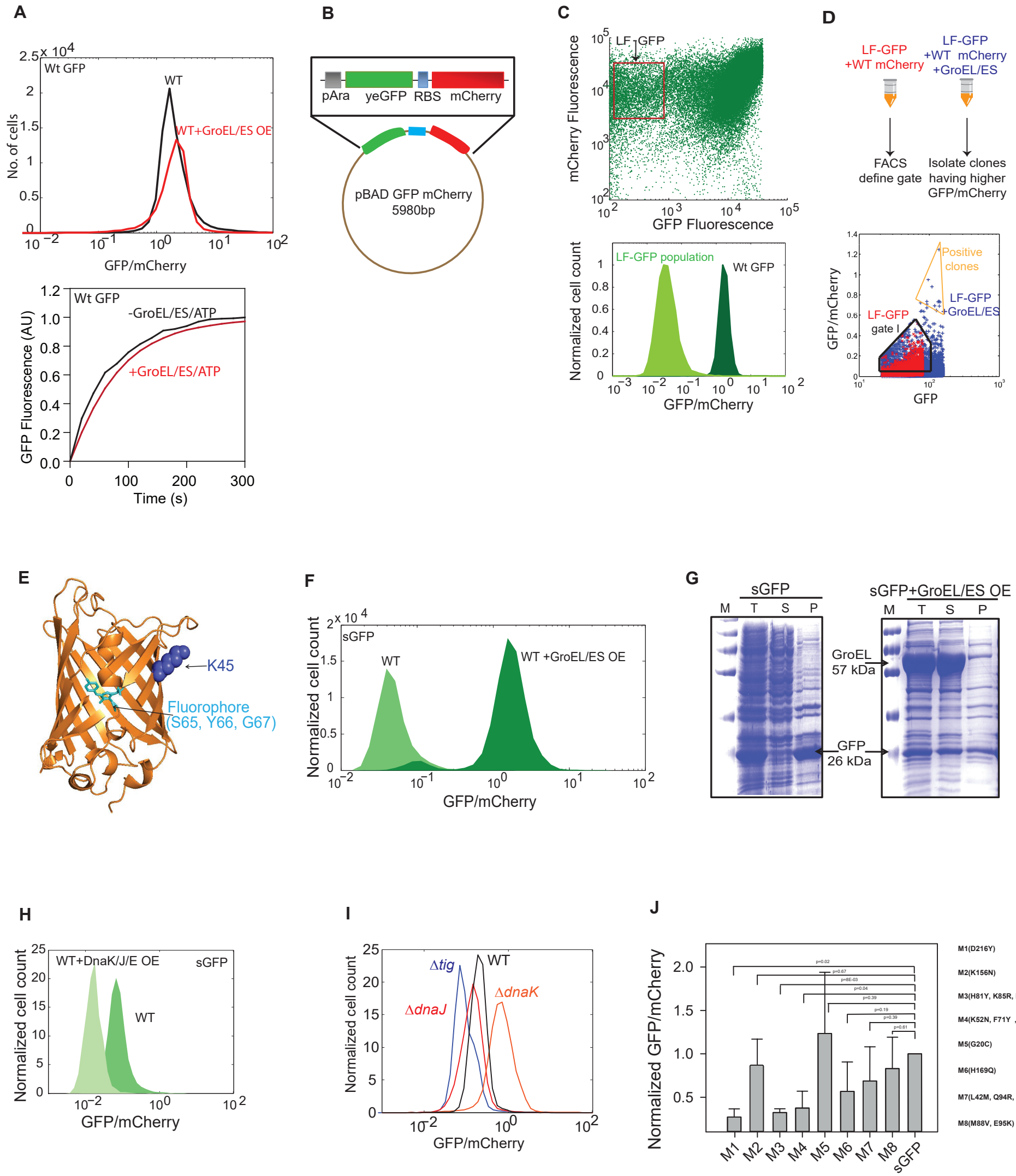
A
Wt GFP
WT
WT+GroEL/ES OE
No. of cells
GFP/mCherry
Wt GFP
-GroEL/ES/ATP
+GroEL/ES/ATP
GFP Fluorescence (AU)
Time (s)
B
pAra
yeGFP
RBS
mCherry
pBAD GFP mCherry
5980bp
C
LF-GFP
mCherry Fluorescence
GFP Fluorescence
LF-GFP population
Wt GFP
Normalized cell count
GFP/mCherry
D
LF-GFP
+WT mCherry
LF-GFP
+WT mCherry
+GroEL/ES
FACS
define gate
Isolate clones
having higher
GFP/mCherry
Positive
clones
LF-GFP
gate I
LF-GFP
+GroEL/ES
GFP/mCherry
GFP
E
K45
Fluorophore
(S65, Y66, G67)
F
sGFP
WT
WT +GroEL/ES OE
Normalized cell count
GFP/mCherry
G
sGFP
sGFP+GroEL/ES OE
M
T
S
P
GroEL
57 kDa
GFP
26 kDa
H
WT+DnaK/J/E OE
sGFP
WT
Normalized cell count
GFP/mCherry
I
Δtig
WT
ΔdnaJ
ΔdnaK
Normalized cell count
GFP/mCherry
J
Normalized GFP/mCherry
M1(D216Y)
M2(K156N)
M3(H81Y, K85R, N105D, L119I)
M4(K52N, F71Y , A206T, G228D)
M5(G20C)
M6(H169Q)
M7(L42M, Q94R, K101E)
M8(M88V, E95K)
M1
M2
M3
M4
M5
M6
M7
M8
sGFP

FIGURE 2

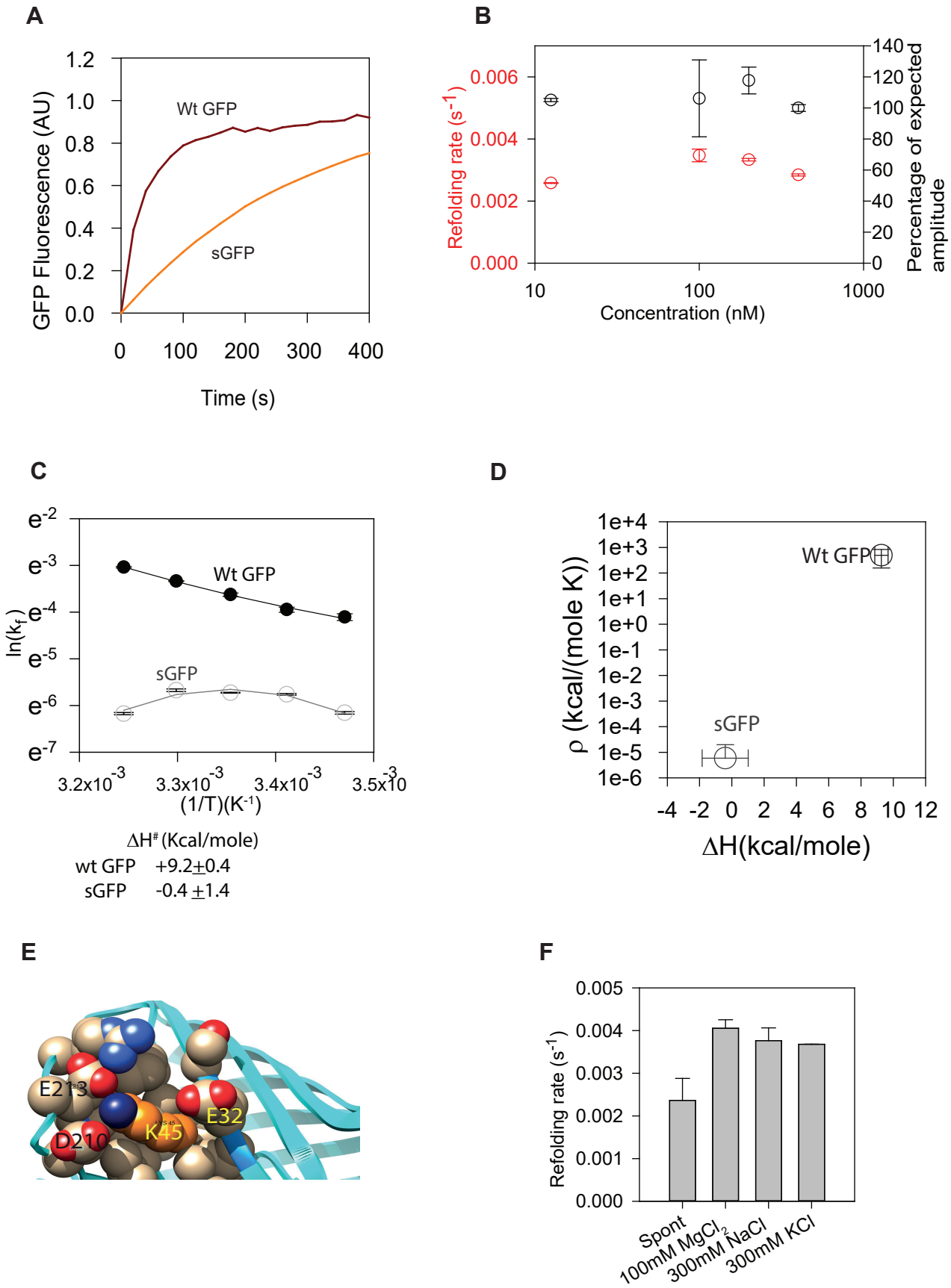
A
GFP Fluorescence (AU)
Time (s)
Wt GFP
sGFP
B
Refolding rate (s-1)
Percentage of expected amplitude
Concentration (nM)
C
ln(kf)
(1/T)(K-1)
Wt GFP
sGFP
ΔH# (Kcal/mole)
wt GFP +9.2±0.4
sGFP -0.4 ±1.4
D
ρ (kcal/(mole K))
ΔH(kcal/mole)
Wt GFP
sGFP
E
E213
D210
K45
E32
F
Refolding rate (s-1)
Spont
100mM MgCl2
300mM NaCl
300mM KCl

Figure 3

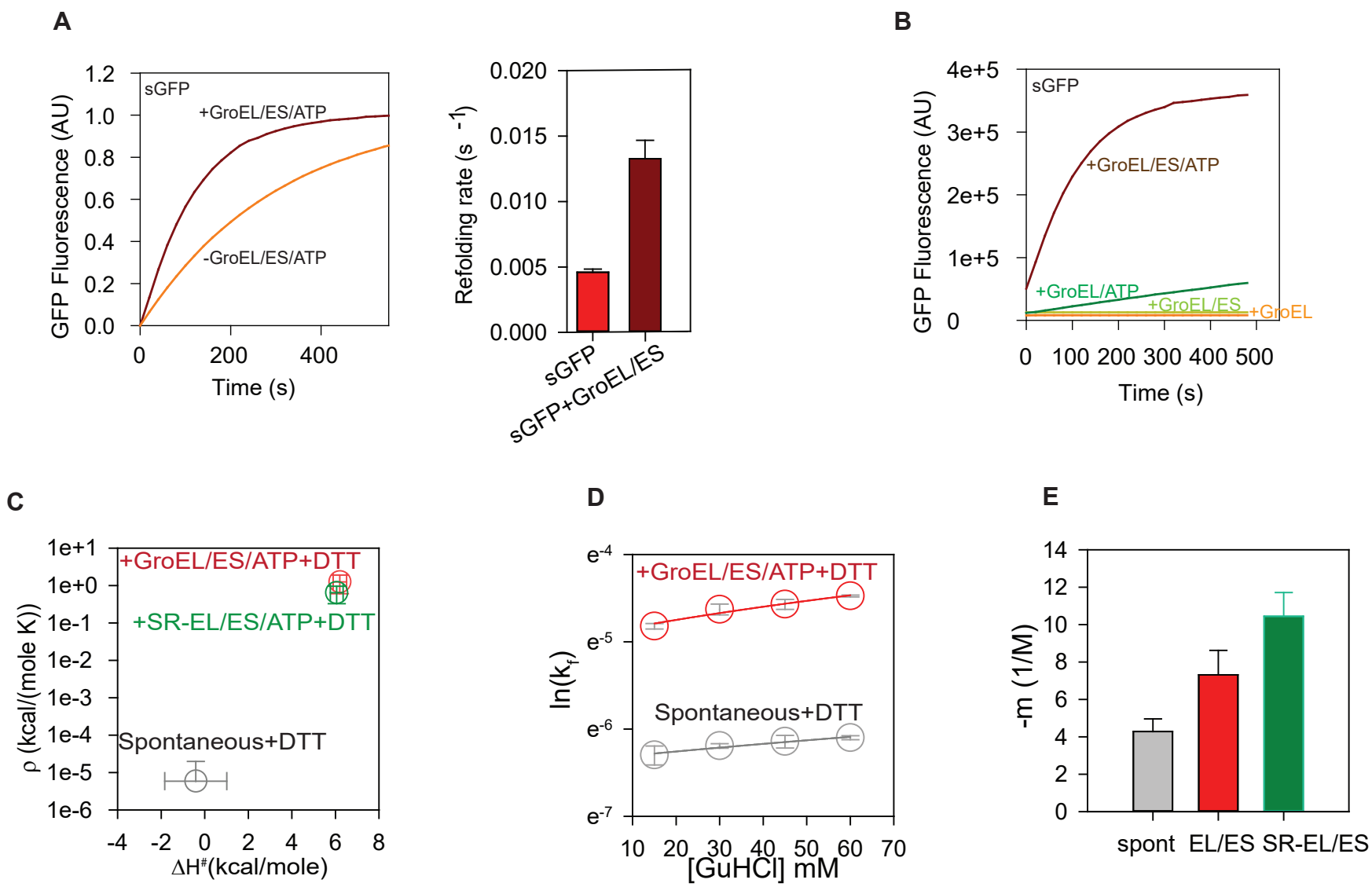
A
sGFP
+GroEL/ES/ATP
-GroEL/ES/ATP
GFP Fluorescence (AU)
Time (s)
Refolding rate (s -1)
sGFP
sGFP+GroEL/ES
B
sGFP
+GroEL/ES/ATP
+GroEL/ATP
+GroEL/ES
+GroEL
GFP Fluorescence (AU)
Time (s)
C
+GroEL/ES/ATP+DTT
+SR-EL/ES/ATP+DTT
Spontaneous+DTT
ρ (kcal/(mole K))
ΔH#(kcal/mole)
D
+GroEL/ES/ATP+DTT
Spontaneous+DTT
ln(kf)
[GuHCl] mM
E
-m (1/M)
spont
EL/ES
SR-EL/ES

FIGURE 4

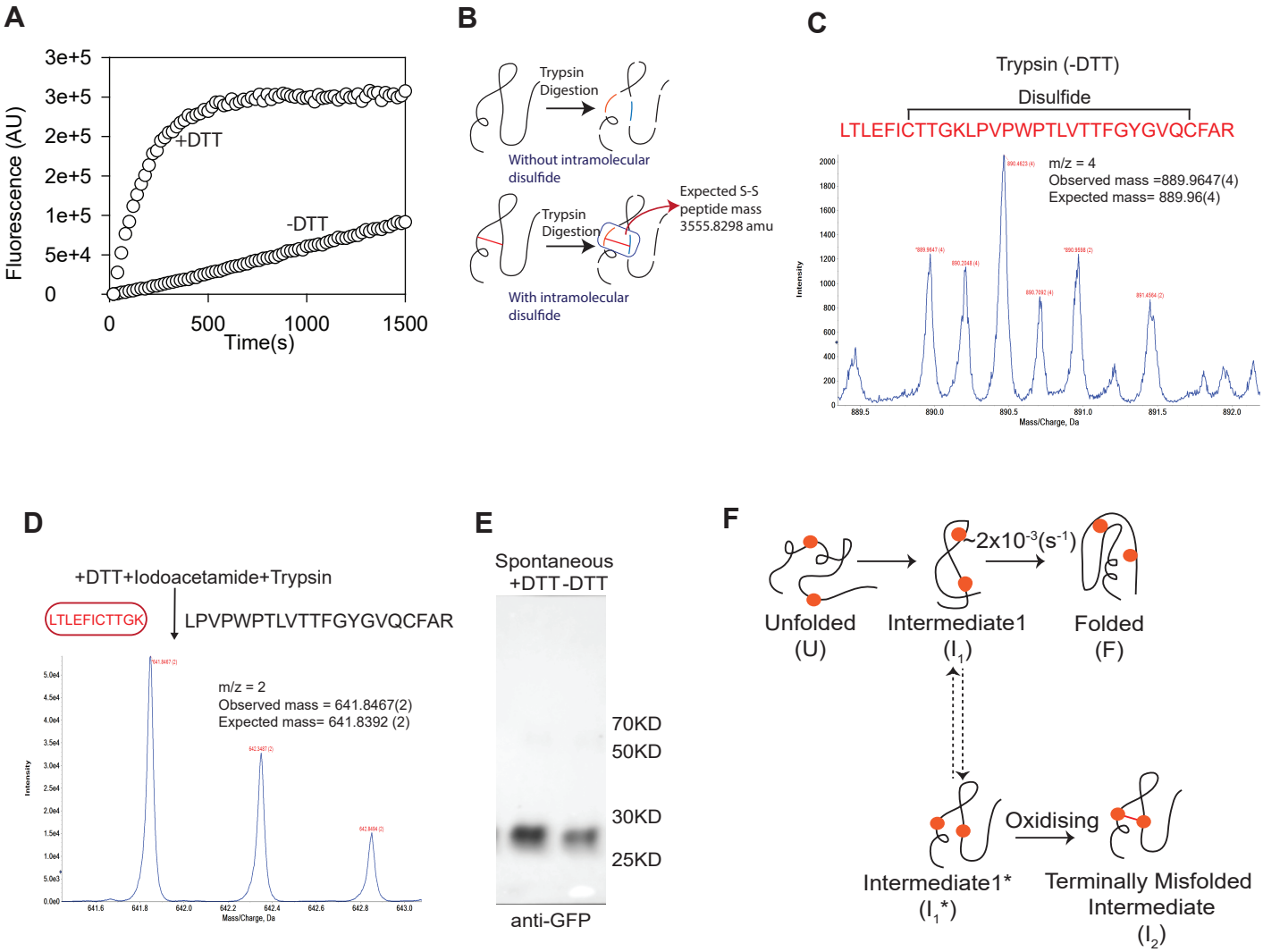
A
Fluorescence (AU)
3e+5
3e+5
2e+5
2e+5
1e+5
5e+4
0
+DTT
-DTT
0
500
1000
1500
Time(s)
B
Trypsin
Digestion
Without intramolecular disulfide
Trypsin
Digestion
With intramolecular disulfide
Expected S-S peptide mass 3555.8298 amu
C
Trypsin (-DTT)
Disulfide
LTLEFICTTGKLPVPWPTLVTTFGYGVQCFAR
m/z = 4
Observed mass =889.9647(4)
Expected mass= 889.96(4)
Intensity
Mass/Charge, Da
D
+DTT+Iodoacetamide+Trypsin
LTLEFICTTGK
LPVPWPTLVTTFGYGVQCFAR
m/z = 2
Observed mass = 641.8467(2)
Expected mass= 641.8392 (2)
Intensity
Mass/Charge, Da
E
Spontaneous
+DTT -DTT
70KD
50KD
30KD
25KD
anti-GFP
F
~2x10-3(s-1)
Unfolded
(U)
Intermediate1
(I1)
Folded
(F)
Oxidising
Intermediate1*
(I1*)
Terminally Misfolded
Intermediate
(I2)

FIGURE 5

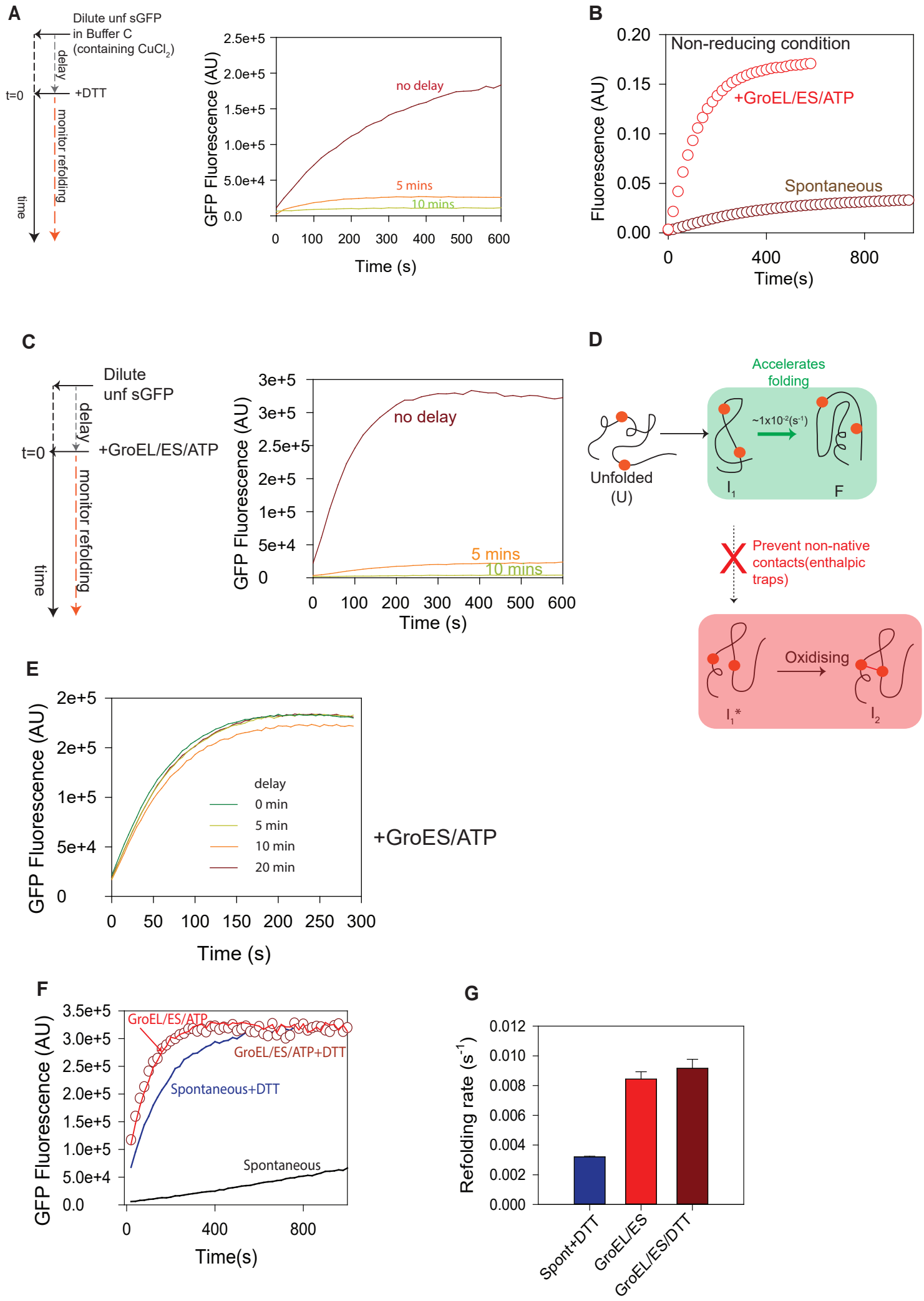
A
Dilute unf sGFP in Buffer C (containing $CuCl_2$)
delay
t=0
+DTT
monitor refolding
time
GFP Fluorescence (AU)
no delay
5 mins
10 mins
Time (s)
B
Non-reducing condition
+GroEL/ES/ATP
Spontaneous
Fluorescence (AU)
Time(s)
C
Dilute unf sGFP
delay
t=0
+GroEL/ES/ATP
monitor refolding
time
GFP Fluorescence (AU)
no delay
5 mins
10 mins
Time (s)
D
Accelerates folding
~1x10-2(s-1)
Unfolded (U)
I1
F
Prevent non-native contacts(enthalpic traps)
Oxidising
I1*
I2
E
GFP Fluorescence (AU)
delay
0 min
5 min
10 min
20 min
+GroES/ATP
Time (s)
F
GroEL/ES/ATP
GroEL/ES/ATP+DTT
Spontaneous+DTT
Spontaneous
GFP Fluorescence (AU)
Time(s)
G
Refolding rate (s-1)
Spont+DTT
GroEL/ES
GroEL/ES/DTT

FIGURE S1

A. GFP/mCherry of different GroEL/ES dependent clones isolated by FACS

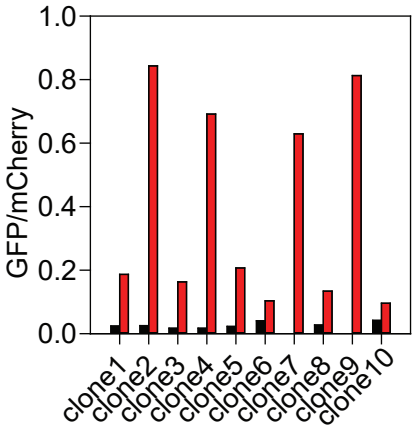

B Native baseline

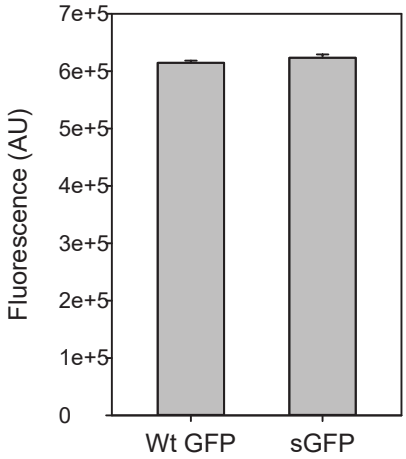

C. Fluorescence of GFP and mCherry channel upon expressing sGFP in the presence and absence of GroEL/ES overexpression

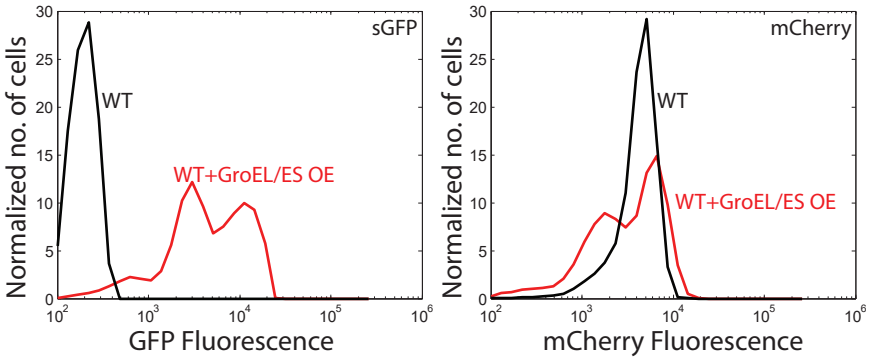

D. Fluorescence of GFP and mCherry channel upon expressing sGFP in the presence and absence DnaK/J/E overexpression

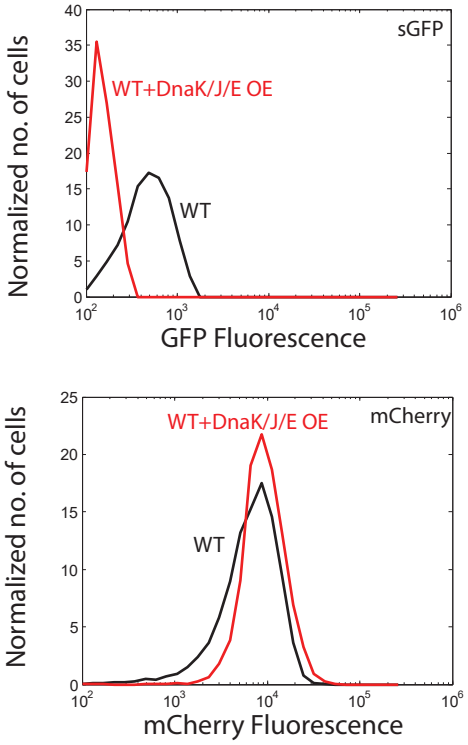

E. Fluorescence of GFP and mCherry channel upon expressing sGFP in the presence and absence of chaperones

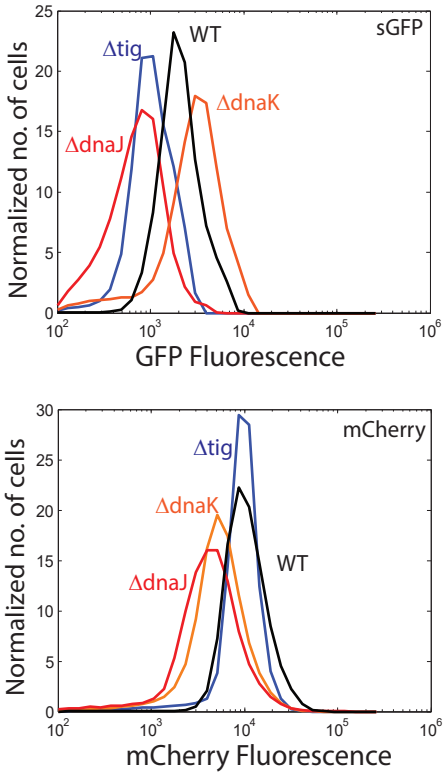

FIGURE S2

A. Unfolding kinetics of sGFP in 6M GuHCl

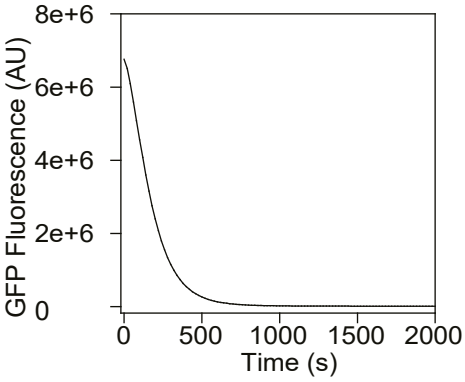

B. Refolding kinetics of sGFP with single exponential fit and residuals

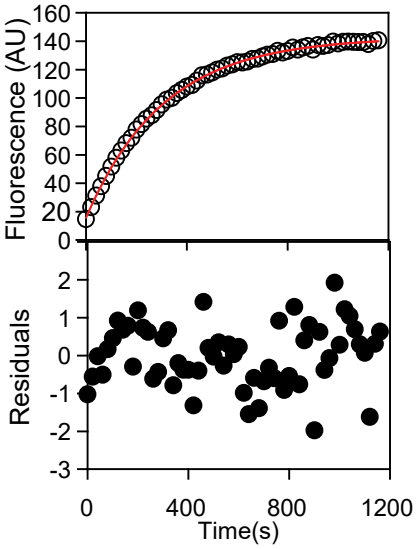

C. Raw spontaneous refolding traces of sGFP at different concentrations.

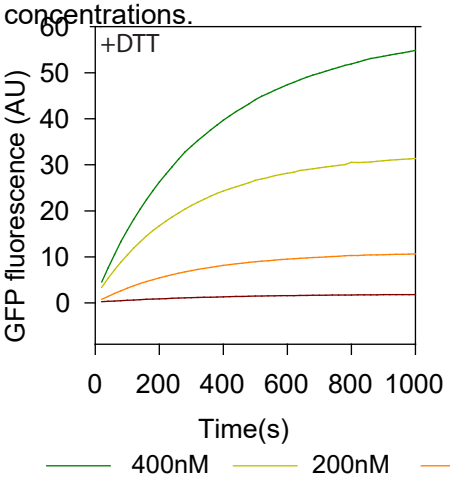

D. Normalized spontaneous refolding traces of sGFP at different concentrations.

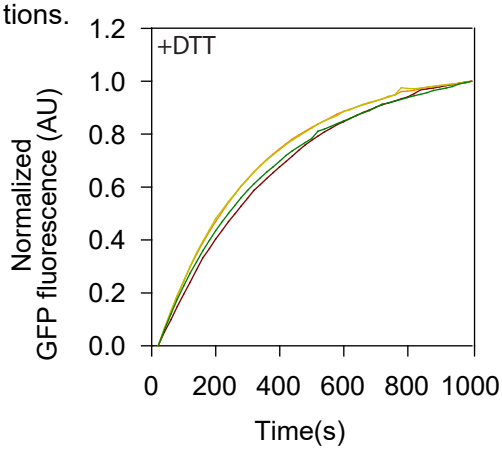

E. Refolding rate of sGFP and Wt GFP in increasing salt concentrations

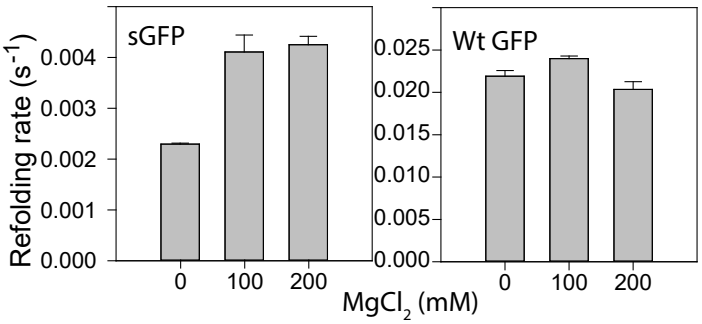

FIGURE S3

A Schematic of an enthalpic barrier in folding funnel

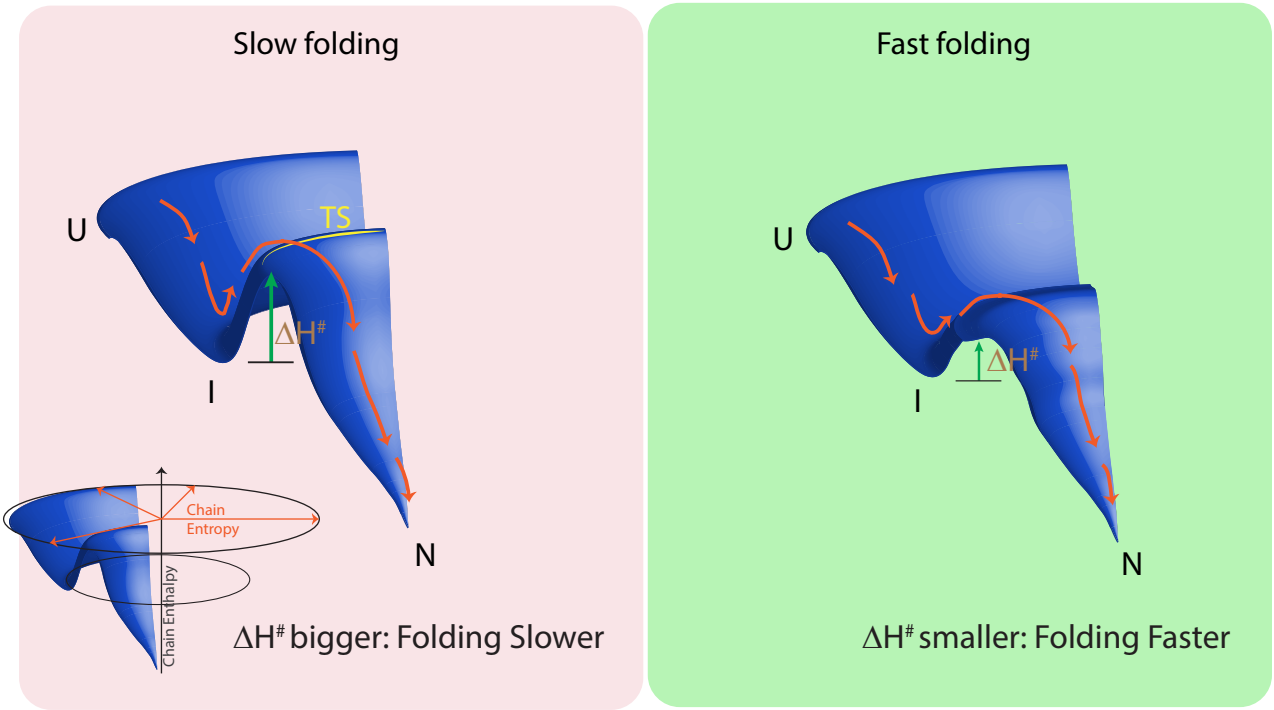

Schematic of an entropic or diffusion-limited barrier in folding funnel (flatness factor)

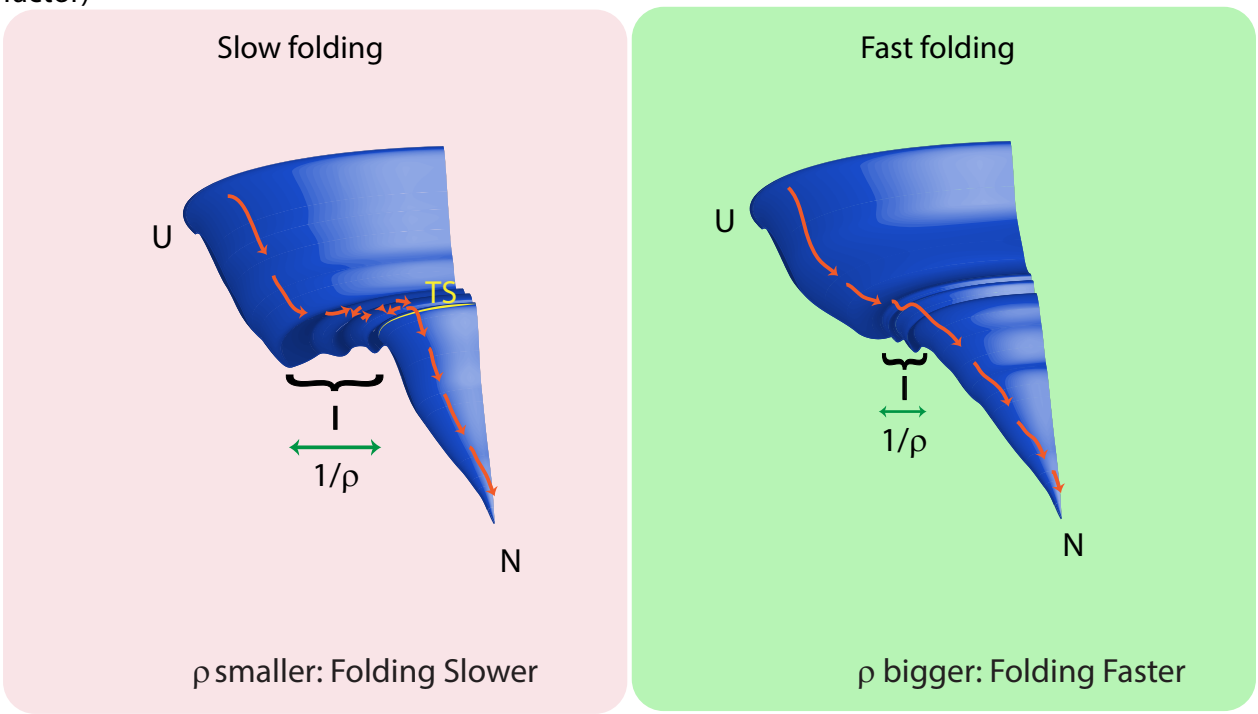

B. Refolding kinetics of sGFP in the presence and absence of DnaK/J/E

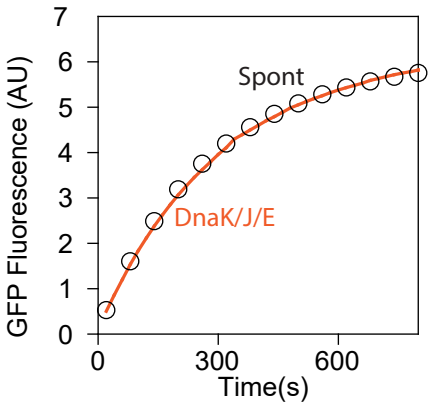

FIGURE S4

A. Effect of $CuCl_2$ on spontaneous folding of sGFP in non-reducing conditions

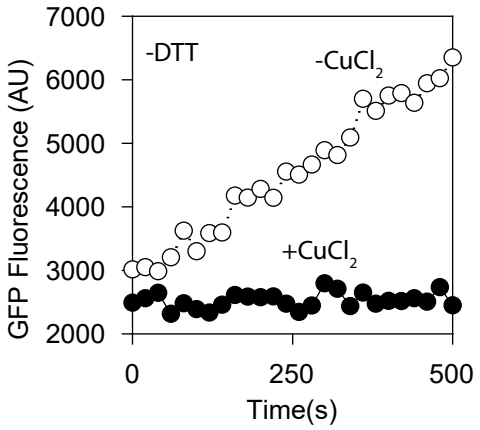

B.Distancebetween the cysteine residues in the native state

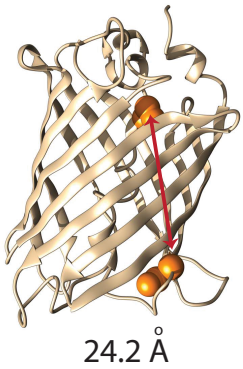

C. Strategy for detecting disulfide formed during sGFP refolding

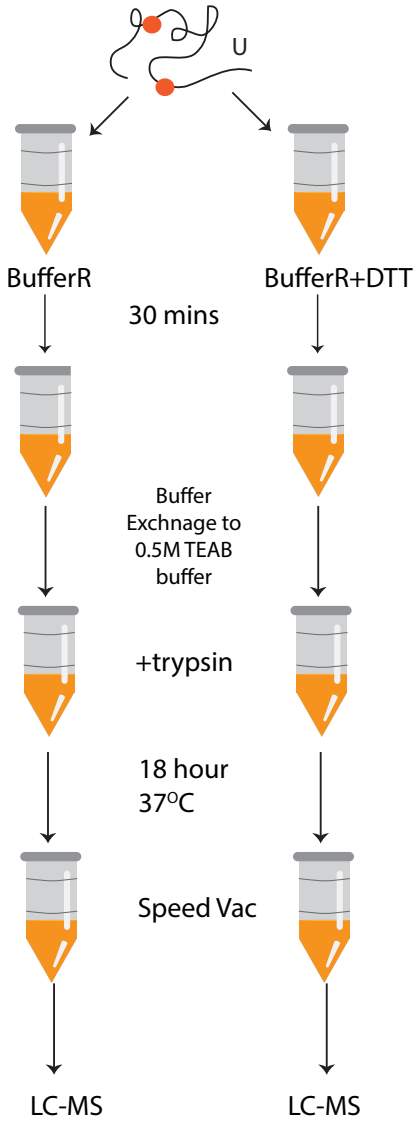

D. Qualitative simplified energy land-scape comparing spontaneous refolding in oxidizing and reducing conditions

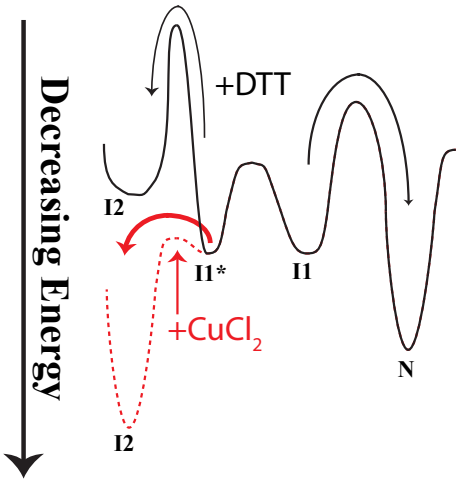

FIGURE S5

A. sGFP refolding in oxidizing conditions in the presence of different components of the GroEL/ES/ATP system

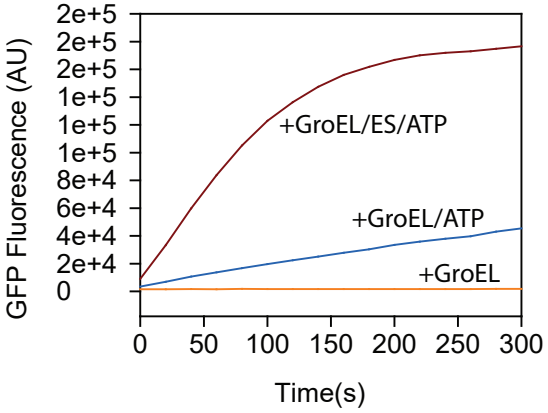

B. Refolding rate as a function of delay in addition of GroES/ATP to GroEL-bound sGFP

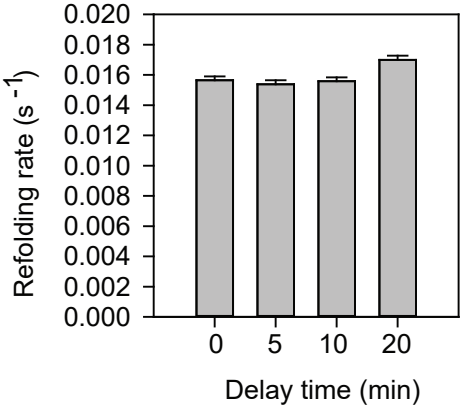

C. Refolding yield of GroEL-bound unfolded sGFP upon addition of GroES/ATP after different delay times

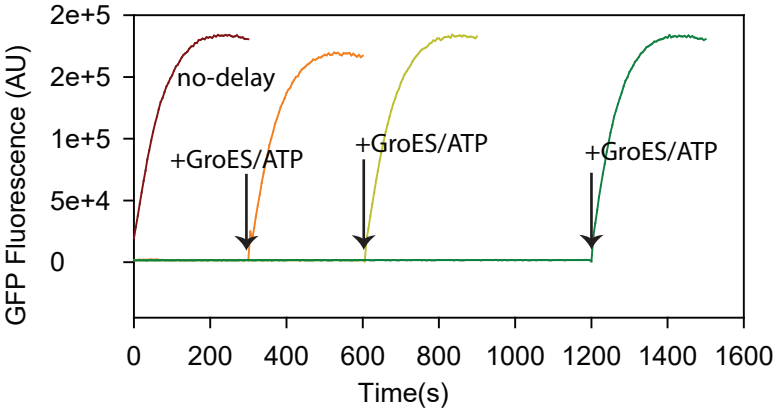

D. Spontaneous refolding rates of sGFP in different concentrations of DTT

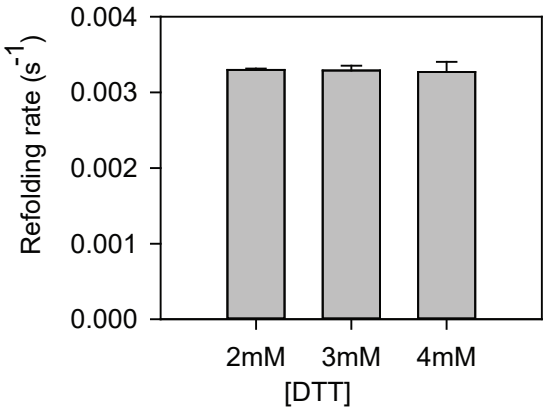

E. Comparison of refolding rate of Wt GFP with and without DTT

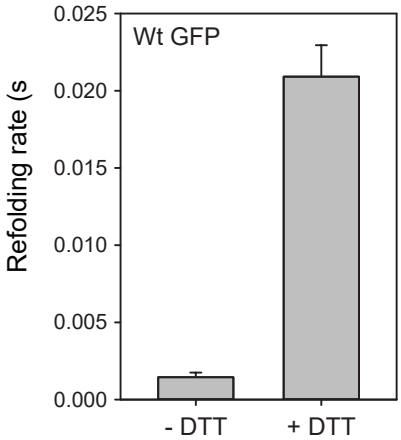

Table S1. Relative quantitation and enrichment of the peptide fragment LTLEFICTTGK that is obtained from the non-disulfide bonded sGFP in refolding reactions with and without DTT. Normalization of the area of the peptide Ion count (IC) is normalized with the area under Total Ion Count (TIC) of both the LS-MS runs.

Sample	Total TIC area	area of LTLEFICTTGK	TIC area normalized	Enrichment (+DTT/-DTT)
sGFP (spont)	3.28E+10	4.74E+05	1.44E-05	---
sGFP+DTT (spont)	1.36E+10	2.15E+07	1.58E-03	109.3

Table S2. Fitted parameters from Arrhenius analysis of temperature dependent refolding reactions in different conditions as given in first column. The standard errors reported are errors obtained after fitting the triplicates of refolding rates obtained at different temperatures for each of the conditions.

Refolding Condition	$\Delta H^{\#}$ (kCal/mole)	Std error ($\Delta H^{\#}$)	$\Delta Cp^{\#}$ (kCal/K)	Std error ($\Delta Cp^{\#}$)	ρ (kCal/(mole.K))	Std error (ρ)
Spontaneous (+DTT)	-0.41	1.42	1.70	0.4505	5.88e-6	1.40e-5
GroEL/ES/ATP	6.20	0.31	-0.18	0.1	1.26	0.65
yHsp60/10/ATP	3.66	0.54	-0.01	0.18	5.14e-3	4.68e-3
hHsp60/10/ATP	0.37	1.05	0.42	0.34	1.44e-5	2.53e-5
y-EL/ES/ATP	5.33	0.27	0.05	0.08	0.1	0.04
h-EL/ES/ATP	4.56	0.26	-0.13	0.08	0.03	0.01
wtGFP (spontaneous)	9.26	0.41	-0.24	0.12	497.30	339.40